REPORT DOCUMENTATION PAGE

Form Approved OMB No. 0704-0188

1. AGENCY USE ONLY (Leave blank)	2. REPORT DATE	3. REPORT TYPE AND DATES COVERED
	July 1993	Final Report

4. TITLE AND SUBTITLE

Assessment of Low-Speed, High Lift Capability of "Diamond" Planform Wings with Mach & Reynolds Number Effects & Possible Improvements

5. FUNDING NUMBERS

F6170893W0560

6. AUTHOR(S)

R.K. Nangia

7. PERFORMING ORGANIZATION NAME(S) AND ADDRESS(ES)

Nangia Aero Research Associates
Consulting Engineers
Maggs House
78 Queens Road
Bristol BS8 1QX, England

8. PERFORMING ORGANIZATION REPORT NUMBER

SPC-93-4023

9. SPONSORING/MONITORING AGENCY NAME(S) AND ADDRESS(ES)

EOARD
PSC 802 BOX 14
FPO 09499-0200

10. SPONSORING/MONITORING AGENCY REPORT NUMBER

SPC-93-4023

11. SUPPLEMENTARY NOTES

Four attachments.

12a. DISTRIBUTION/AVAILABILITY STATEMENT

Unlimited

12b. DISTRIBUTION CODE

13. ABSTRACT (Maximum 200 words)

As a result of USAF-EOARD sponsored "Window-on-Science" visit to WL and AFOSR (Apr 92, Ref 1) several areas of mutual interest were identified (refs 2 and 3). One of the aspects concerning high lift development on highly tapered "diamond" type ("stealthy") planforms is being currently undertaken under the part sponsorship of the USAF-EOARD.

For reasons of stealth, highly tapered wings of "diamond" planform are being actively pursued for practical application on advanced fighter aircraft. Such wings are known to be prone to flow separations at the wing tip. The underlying philosophy of the work program on this class of aircraft is to maximize the performance and subsonic-transonic maneuverability within the constraints imposed by low radar signature. LE and TE devices are therefore incorporated and the high lift performance needs to be assessed theoretically and experimentally.

This report highlights two main objectives: (1) to assess the given "diamond" (cambered and twisted) wing with and without LE and TE flaps and (2) to indicate possible improvements. These two objectives lead also to the methodology for dealing with such wings when more accurate design information may be required in future. The premise is that such information will lead to an appreciation of compromises between constraints imposed by radar signature considerations and aerodynamic performance.

14. SUBJECT TERMS

15. NUMBER OF PAGES

96

16. PRICE CODE

17. SECURITY CLASSIFICATION OF REPORT	18. SECURITY CLASSIFICATION OF THIS PAGE	19. SECURITY CLASSIFICATION OF ABSTRACT	20. LIMITATION OF ABSTRACT
UNCLASSIFIED	UNCLASSIFIED	UNCLASSIFIED	UL

TECHNICAL REPORT

RKN/AERO/Report/93-50
Issue 1
July 1993

ASSESSMENT OF LOW-SPEED, HIGH LIFT CAPABILITY OF "DIAMOND" PLANFORM WINGS WITH MACH & REYNOLDS NUMBER EFFECTS & POSSIBLE IMPROVEMENTS

R. K. Nangia

SUMMARY

For reasons of stealth, highly tapered wings of "Diamond" planform are being actively pursued for practical application on advanced fighter aircraft. Such wings are known to be prone to flow separations at the wing tip. The underlying philosophy of the work programme on this class of aircraft is to maximise the performance and subsonic-transonic manoeuvrability within the constraints imposed by low radar signature. LE and TE devices are therefore incorporated and the high lift performance needs to be assessed theoretically and experimentally.

This report highlights two main objectives: (1) to assess the given "diamond" (cambered and twisted) wing with and without LE and TE flaps and (2) to indicate possible improvements. These two objectives lead also to the methodology for dealing with such wings when more accurate design information may be required in future. The premise is that such information will lead to an appreciation of compromises between constraints imposed by radar signature considerations and aerodynamic performance.

The techniques have shown the capability to predict the lift-drag polar with sufficient accuracy to enable derivation of the LE & TE flap schedules including LE radius, Mach and Reynolds number effects.

For a wing with scheduled LE and TE flaps, the benefits of rounded LE are apparent at high lift. Increasing Reynolds number (flight conditions) adds to the benefits. It is expected that for the same performance, a sharp LE wing will in general, require a higher LE deflection and the deflection schedule will need to be kept finely "tuned". On the other hand, a small amount of rounding on LE allows a much more tolerant deflection schedule.

The technique will assist with the assessment of flight manoeuvrability and its enhancement. The work will allow the design or aircraft updating cycle to commence with a good idea of the relative effectiveness of the various geometries. In view of the encouragement gained, further theoretical and experimental work has been recommended in several areas. These should have a constructive and practical impact on current and future combat aircraft

Nangia Aero Research Associates
Consulting Engineers
Maggs House
78 Queens Road
Bristol BS8 1QX, UK

The Investigation which is the subject of this report has been, in part, supported by the USAF-EOARD, London, UK, under Contract SPC-93-4023. This is gratefully acknowledged.

DISTRIBUTION LIST

1 Lt Col. Al Janifzewski Technical Director, USAF-EOARD,
223-231 Old Marylebone Road,
LONDON, NW1 5TH, UK

1 Dr. Mark Maurice Chief Aeronautical Engineering, USAF-EOARD,
223-231 Old Marylebone Road,
LONDON NW1-5TH, UK

1 Major D. Fant AFOSR/NA, Bolling AFB, DC 20332-6448, USA

1 Mr. R. F. Osborn Leader FIMM, USAF-WL, AFB, OHIO 45433-6523, USA

1 Dr. W. Calarese Directorate, USAF-WL, AFB, OHIO 45433-6523, USA

1 Dr. D. Multhopp WL/FIGC, USAF-WL, WPAFB, OHIO 45333-7913

1 Dr. J. Luckring NASA Langley Research Center
Mail stop 361, Hampton VA 23665-5525

1 Dr. Lawrence Olson NASA Ames Research Center
Mail stop 247-1, Moffet Field CA 94035

1 Dr. Marvin Walters NAW CADWAR
Code 6051, Warminster PA 18974

1 Dr. James Olsen Chief Scientist
Flight Dynamics Directorate, WL/FI-3,
Wright-Patterson AFB OH 45433-7531, USA

1 Mr. Louis J Williams Director, High Speed Research Div.
Office of Aeronautics & Space Technology
NASA (Code RJ), Washington DC 20546

1 Dr. R.K. Nangia (Author) Consulting Engineer, Bristol, UK

CONTENTS

1. INTRODUCTION

1.1. Background

As a result of USAF-EOARD sponsored "Window-on-Science" visit to WL and AFOSR (April' 92, Ref.1), several areas of mutual interest were identified (Refs.2 and 3). One of the aspects concerning high lift development on highly tapered "diamond" type ("stealthy") planforms is being currently undertaken under the part sponsorship of the USAF-EOARD.

1.2. High Lift Development of Modern "Stealthy" Aircraft

Fig.1.1 shows a view of the class of aircraft (ACWFT) under consideration which follow on from the F-22 and F-23 arrangements. Fig.1.2 gives three views of a related configuration without vertical surfaces. The "chined" lifting body is fully integrated with the wing and inlet. The "diamond" planform wing has LE sweep of 40°, and TE sweep of −30°. Such wings, because of high taper, are prone to flow separations at the wing tip. The underlying philosophy of the work programme on this class of aircraft is to maximise the performance and subsonic-transonic manoeuvrability within the constraints imposed by low radar signature. LE and TE devices are therefore incorporated and the high lift performance needs to be assessed theoretically and experimentally.

Such configurations are being tested in various wind tunnel facilities in the USA to obtain low-speed longitudinal and lateral information with varying Mach and Reynolds number effects:

7x10 ft NASA Ames, Mach 0.18, q=50 psf
0.267 scale half model representing the exposed wing panel.
0.100 scale full model.

40x80 ft NASA Ames, Mach 0.4, q=215 psf
0.55 scale full model.

80x120 ft NASA Ames, Mach 0.09, q=30 psf
0.55 scale full model.

Naturally, because of inevitable time and cost restraints, not all possible combinations of geometry can be tested in the wind tunnels. Therefore a need for supporting, project-biased, theoretical work (rather than CFD), has been identified. In the first instance, the techniques seek to compare results with those from experimental work. Once a reasonable confidence level has been demonstrated, the theory will enable an expansion of the database. It will enable also the identification of the promising areas for further CFD and experimental activities.

1.3. Objectives of the Present Work Programme & Techniques Used

The main objectives of the present work programme are **two**-fold. The **first** objective is to assess the given "diamond" (cambered and twisted) wing with and without LE and TE flaps. The **second** objective is to indicate possible improvements. These two objectives lead also to the methodology for dealing with such wings when more accurate design information may be required in future. Such information will lead to an appreciation of compromises between constraints imposed by radar signature considerations and aerodynamic performance.

The techniques based on lifting surface and panel methods have been developed and refined over the last few years. They allow predictions of forces and moments arising on fairly general (and complete) configurations having thick or thin wings with and without LE and TE flaps. The methods incorporate attained thrust principles for the given flow parameters: Mach number and Reynolds number. Previous applications of the theory to a wide

variety of "conventional" wings have demonstrated very close and encouraging agreement with experiment.

1.4. Layout of This Report

The remainder of this report is presented in **Sections 2 to 8** as follows:

Section 2 deals with configuration geometry highlighting the exposed wing and whole geometry differences.

Section 3 presents results for exposed wing (with and without LE and TE flap deflections) and assesses the effects of introducing variations of LE radius and Reynolds number. Comparisons with Experiment are given at Mach 0.18.

With the encouragement gained from the comparisons in Section 3, **Section 4** presents predicted results on the LE flap chord variation on the exposed wing configuration at Mach 0.18.

Section 5 introduces predictions for Mach 0.4.

Section 6 presents predictions for a wing+body arrangement and assesses the effects of introducing variation of LE radius.

Section 7 describes the scope of further work required.

In **Section 8**, Concluding Remarks have been presented.

2. CONFIGURATION GEOMETRY, ASSUMPTIONS & FLOW PARAMETERS

For the class of configuration typified in Figs.1.1 and 1.2, the only geometric details available to us were for the exposed Basic wing (CONFIG-A) as illustrated in Fig.2.1. A half-model of this wing (semi-span 4.27 ft) was tested in the NASA Ames 7x10 ft wind tunnel at 0.267 scale. The wing has LE sweep of 39.51° and TE sweep -40.60°, thus different from that in Fig.1.2. The leading edges of the basic wing were sharp. LE and TE flaps are also featured.

During the later stages of the test programme, the LE of the wing was rounded in a simple fashion. Selected tests were undertaken with LE radii (r_n = 0.1875" and 0.375", i.e. assumed to be normal to the LE and independent of the spanwise distance). For these tests therefore r/c along the wing-span varies considerably (very much higher at the wing-tip). Further details of the resulting aerofoil sections are not available to us at this stage.

The emphasis of the studies is on improving the understanding of the wing aerodynamics. However, in view of the compact-integrated nature of the overall configuration and the presence of a lifting body, we needed to represent the fuselage effects in a realistic, although simplified manner. Fig.2.2 illustrates the model (CONFIG-B) that we have adopted which represents the essential features of the body and wing intersection. The body is assumed to be uncambered at this stage. Grid optimisations have not been undertaken.

The following table compares the exposed (CONFIG-A) and gross wing on CONFIG-B.

Geometry Parameters

The wing planform parameters based on exposed wing semi-span=1.0 are as follows:

	Exposed		Gross
Aspect Ratio	2.0049		2.1220
Wing Area S	0.99756		2.2419
semi-span	1.0		1.54394
c_r	1.8384		2.7505
c_t		0.1567	
c_{av} = c	0.99756		1.4536
Taper ratio	0.08523		0.06971

LE Sweep	39.51°
¼ chord sweep	22.23°
TE Sweep	-40.60°

Wing Aerofoil t/c ≈ 4.5%, reference case with sharp LE (r/c=0.0)
Maximum t/c at 0.396c on cambered and twisted sections.

LE Shape

The predictive technique allows aerofoil parameters to be chosen and the most significant parameter is r/c variation along the span. In the present programme of work, "regular" variations of r/c ranging from 0.0 to 0.0022 have been considered in addition to the "non-linear" r/c variations along the span (r_n = 0.1875" and 0.375").

LE Flap (LEF) Deflection

0°, 15° , 30° , 45° (normal to LE)
0°, 11.78°, 24.19°, 37.89° (chordwise)

TE Flap & Aileron (TEF inner & outer), usually deflected together

0°, 15° inner & outer (normal to LE)
0°, 10.66° inner, 11.62° outer (chordwise)

Configuration Notation

For convenience, the configuration notation is in terms of LEF/TEF.

Flow Parameters

Test Mach No	Reynolds No R (based on c_{av})			
0.09	5.37×10^6	(0.550 model),	10.06×10^6	(flight)
0.18	1.95×10^6	(0.100 model),	19.54×10^6	(flight)
0.18	5.22×10^6	(0.267 model),	19.54×10^6	(flight)
0.40	23.89×10^6	(0.550 model),	44.71×10^6	(flight)

For convenience, we have chosen a more "regular" set of Reynolds numbers for calculations i.e. R = 2, 5, 10, 20 and 50 $\times 10^6$.

3. CALCULATIONS ON EXPOSED WING (CONFIG-A) & COMPARISONS WITH EXPERIMENT AT Mach 0.18

As mentioned in Section 2, the technique can allow different LE shapes to be evaluated with comparative ease. Several possibilities exist for choosing the LE radius variations along the span. In the early stages of the work programme, for the sake of simplicity, r/c values were held constant along the wing-span. In the later stages, r_n = 0.1875" and 0.375" were studied which emphasises large r/c at the wing-tip.

The techniques can allow for a relaxed TE wake. Since it is time and effort intensive, it was not considered practical to perform this at all

incidences of interest. However, specimen cases were investigated at high α. These showed that lift coefficient was increased by about 0.05 to 0.1 at about 24° incidence compared with the equivalent case for unrelaxed TE wake. There were however, no perceived differences in drag polars. If required in future studies, TE wakes can be relaxed.

Similarly, viscid effects can be allowed for in an empirical way, if required, in future investigations. Our experience is that such effects become more important on thicker wings. The viscid effects will tend to reduce lift at higher incidences.

In the present calculations, the emphasis is on locating the first "break" in the lift and drag relationships. Vortex breakdown effects (second "break") are related directly to the first "break". Experience suggests that delaying the first "break", in general, also delays the second "break". From the point of view of deriving the actual operating schedule for a wing with LE and TE flaps, as will be seen later, the vortex breakdown effects become relatively less significant as the LE flap deflection progressively increases or LE radius increases. However, an early assessment of the vortex breakdown effects was made on the basic wing without LE and TE flap deflections on which these effects dominate.

3.1. Basic Wing, LE & TE Flaps Undeflected

Figs.3.1-3 show the results for the basic wing (LEF/TEF: 0/0) with LE radius variation (r/c = 0.0001, 0.001 and 0.0022) for three Reynolds numbers: 2, 5 and 20 $x10^6$. The relationships depicted through representative α ranges are:

$$C_N - \alpha \ , \ C_{Ai} - \alpha \ , \ C_{Di} - C_L \ , \ C_L - \alpha \ , \ C_{Di} - \alpha \text{ and } k - C_L$$

The lift induced drag factor 'k' for a wing of aspect ratio (A) follows from the conventional simple definition of drag coefficient (C_D) in terms of the surface friction (C_{D0}) and lift dependent (C_{Di}) components as:

$$C_D = C_{D0} + C_{Di}$$

$$k = \pi A C_{Di}/C_L^2 = \pi A (C_D - C_{D0})/C_L^2.$$

The above definition ignores the small contribution due to lift effects on C_{D0}.

The theoretical results show curves for 0% and 100% LE suction as well as for the Mach and Reynolds number effects. The 0% LE suction curves correspond to the case of sharp LE i.e. r/c = 0.0. From our experience, the C_{Ai} and k variations indicate the break points and flow separation trends in a more obvious fashion which are very important in assessing the performance of wings.

Fig.3.4 depicts the results for Reynolds number variation (R = 2, 5 and 20 $x10^6$) with LE radius set at r/c = 0.0022.

From these figures, the first "breaks" give the main trends:

1. Wing has positive lift at zero α due to the presence of small TE camber.

2. Rounding of the LE has a beneficial effect on drag as Reynolds number increases. The benefit decreases as r/c increases. It is however, physically difficult to achieve very low r/c values and maintain the flows. A more reasonable or useful starting point from practical considerations could be r/c=0.0005.

3. Lift is slightly reduced due to LE rounding at higher α.

4. The best k values attained are of the order 1.0 for the rounded LE. For sharp LE, k = 1.2 is attained at C_L near 0.2. These values appear to be plausible.

Specimen Vortex breakdown studies undertaken with another technique based on that of Lan and Hsu (Ref.4) have shown that the onset of vortex breakdown would be at the TE at around 9-10° incidence. The vortex breakdown will progressively move forward, eventually limiting the maximum lift of the wing. The vortex breakdown limits can be "coerced" and detrimental effects relieved to give high lift capability with deflected LE and TE devices.

3.2. Basic Wing with Deflected LE & TE Flaps

Figs.3.5-7 show the results for the wing (LEF/TEF: 15/15) with LE radius variation (r/c = 0.0001, 0.001 and 0.0022) for three Reynolds numbers: 2, 5 and 20 x10^6. Fig.3.8 shows the results for Reynolds number variation (R = 2, 5 and 20 x10^6) with LE radius r/c = 0.0022.

Figs.3.9-11 shows the results for the wing (LEF/TEF: 30/15) with LE radius variation (r/c = 0.0001, 0.001 and 0.0022) for three Reynolds numbers: 2, 5 and 20 x10^6. Fig.3.12 shows the results for Reynolds number variation (R = 2, 5 and 20 x10^6) with LE radius r/c = 0.0022.

Figs.3.13-15 shows the results for the wing (LEF/TEF: 40/15) with LE radius variation (r/c = 0.0001, 0.001 and 0.0022) for three Reynolds numbers: 2, 5 and 20 x10^6. Fig.3.16 shows the results for Reynolds number variation (R = 2, 5 and 20 x10^6) with LE radius r/c = 0.0022.

We note:

1. The difference (region) between 0% and 100% LE suction curves expands either side of the nearly "attached" region. The magnitude of the difference decreases as LE flap deflection increases. This difference tends to give non-linear appearance to the lift curves.

2. For the sharp LE curve, the C_{L0} value actually decreases as the LE deflection increases. This effect raises the lift-curve slope at small incidences. This is however of little consequence from the point of view of determining LE flap schedule.

3. The best k values attained are of the order 1.13 for the rounded LE. For sharp LE, k = 1.18 is attained.

4. As the LE flap deflection increases, the range (or domain between the lower and higher limits of α or C_L) over which flow might be expected to be attached varies. For sharp LE, the attached flow range is expected to be very small. As the roundness of LE is increased, the attached flow domains expand. A corollary is that higher the upper limit defining the domain is, the higher the α of vortex breakdown onset.

We now take in more detail on the these domains.

Fig.3.17 shows the attached flow domains of α and C_L for r/c = 0.0022. As Reynolds number increases, the domains for a given LEF deflection expand.

Fig.3.18 (a-c) shows the effect of LE radius r/c variation on the attached flow domains of α and C_L for R = 2, 5 and 20 x10^6. As r/c increases, the domains expand.

It follows from these graphs that for the derivation of schedules for LE and TE flaps, it is desirable to operate within these domains. The benefits

of rounded LE are apparent at high lift. Increasing Reynolds number (flight conditions) will lead to added improvements. It is expected that for equivalent performance, a sharp LE wing will in general, require a higher LE deflection and the deflection schedule will need to be kept closely "tuned". On the other hand, even a small amount of rounding on LE allows a much more tolerant deflection schedule. The techniques available allow us to assess these benefits.

Fig.3.19 summarises the effect of LEF and TEF deflections on lift-drag characteristics for sharp LE wings. The C_D - C_L and k - C_L graphs enable the derivation of an operating schedule for LE and TE flaps.

3.3. Comparisons with Selected Results from Tests on A Half-Wing in 7x10 ft Wind Tunnel at Mach 0.18

It is worth mentioning that the half-wing experimental results in form of lift-drag graphs were conveyed to us after most of the predictions were completed and discussed with the technical monitors of the programme. There were some small differences in hinge-line assumptions. The experimental results then enabled the comparative graphs against predictions to be derived.

The half-model tests naturally, imply some reservations as regards the measured forces and moments. For a model with a balance, inevitably, small leakages of flow are likely to occur at the wing intersection with the reflection plate. Further, as the boundary layer develops on the reflection plate this can reduce the effectiveness of the root TE. Therefore some uncertainties can arise in C_{D0} and C_{L0} (at $\alpha = 0°$).

The C_{D0} term is fairly small and from the experiments it is estimated to be of the order of 0.008 for the basic sharp LE wing (strictly the uncambered, untwisted mode). The emphasis of the comparisons is however, on lift-induced drag prediction.

Sharp LE

Fig.3.20 shows the experimental results. These results were digitised from lift and drag graphs. The format of presentation here is similar to that for the predicted results of Fig.3.19. In view of the small uncertainities in C_{D0} and C_{L0} on a half-wing model, any resulting corrections have been omitted at present.

Note that:

1. The basic wing with undeflected LE and TE shows a very early first break and a corresponding early second break. This is as expected on the basis of predictions.

2. The character of C_{L0} variation with LE flap deflection increasing is predicted by theory.

3. The best k values are of the order of 1.0 for the wings with LE and TE flaps deflected. This is somewhat surprising as C_{D0} effects have not been included. If C_{D0} is to be subtracted, k values will then be less than 1.0. This suggests that we need to look towards C_{D0} values from complete wing tests in due course. Overall this is a minor problem in the present context as the various break points can be identified with reasonable confidence.

4. From the C_D - C_L and k - C_L graphs, we can derive the operating schedule for LE and TE flaps. For sharp LE, optimum performance implies that LE flaps are always "tuned". Further improvements at higher C_L are likely with increased LE and TE flap deflections.

Fig.3.21 summarises the lift-drag envelope from theory (Fig.3.19) and experiment (Fig.3.20). It is very encouraging to note that the theoretical predictions are very close to the experimental results. The theory appears capable of predicting the flap schedules, although we have not needed to include all the second-order features of the theory available to us (e.g. relaxed wakes, viscid corrections at the expense of course, of extra complexity). Vortex breakdown effects limits are apparently "pushed" higher by increasing LE flap deflection.

Predicted Effect of Rounded LE (r/c = 0.0022)

It is of interest to see the effect of a rounded LE. Fig.3.22 shows the lift-drag envelope compiled from Figs.3.4, 3.8, 3.12 and 3.16 for R = 5 x10^6. This suggests that the improvements due to LE radius occur mainly at high lift and that the LE flap schedule does not need to be so finely "tuned". Higher LE deflections should lead to further small improvements.

Effect of Rounded (r_n = 0.1875" and 0.375"), Theory & Experiment

As mentioned in Section 2, during the later stages of test programme, the LE of the wing was rounded in a simple fashion. Selected tests were undertaken with LE radii r_n = 0.1875" and 0.375".

Figs.3.23 and 24 show the predicted effect of LE radius changes on two cases of the basic wing with deflected LEF and TEF (LEF/TEF: 30/15 and 45/15).

Fig.3.25 shows the experimental results for the sharp and rounded LE wings for LEF/TEF: 30/15 case. Fig.3.26 refers to LEF/TEF: 45/15 case. We note that rounding of the LE enables higher lift to be attained prior to flow separations. This inference is in line with the comments based on attached flow domains (Section 3.2). It confirms that the benefits of a rounded LE appear at high lift. The vortex breakdown effects are also delayed by a rounded LE.

We can now summarise all the comparisons on the basis of attached flow C_L domains as illustrated in Fig.3.27. The agreement between predictions and experiment for the first break with and without LE radius effects is remarkably encouraging. This once again confirms that theory predicts with reasonable confidence, the LE radius and Reynolds number effects and the attached flow regions.

In the context of high lift, Fig.3.28 compares the C_D - C_L from theory and experiment for the LEF/TEF: 30/15 and 45/15 configuration for LE radii r_n = 0.375". We note that apart from C_{D0} effects already indicated, the predictive method is capable of being used for deriving LEF and TEF schedules.

4. SELECTED PREDICTIONS ON EXPOSED WING (CONFIG-A), Mach 0.18

With the encouragement provided by the foregoing comparisons, it was felt opportune to look at some geometry variations. An important design aspect on very thin wings is that for given control effectiveness, the LE and TE controls need to be minimal in surface area and operate with as small a hinge moment as possible. An estimation of the effects of LE flap chord variation is one of the early questions to be addressed.

4.1. LEF Chord Variation

Fig.4.1 shows a selection of four possible hinge-lines (1 - 4) for the LE flap geometry. Hinge-line (1) is the reference case, as used in the preceding work. For the present purposes, we have chosen to assess the

effects of reducing the flap chord and compare hinge-line (3) against the reference (1). For this exercise, TE Flap was kept undeflected.

Fig.4.2 summarises the attached flow domains of α and C_L with respect to LE flap deflection for the two hinge-lines (r/c = 0.0022, TEF 0°). As Reynolds number increases, the domains expand. The domains are however, narrower and are at a smaller "slope" for hinge-line (3) indicating that:

1. For a given deflection, LE flaps with hinge-line (3) are less effective than those with hinge-line (1). This appears plausible.

2. For equivalent effectiveness, hinge-line (3) flaps will require increased deflection (approximately 5°-10° more). TE flap deflection can be introduced to increase lift.

3. From the point of view of minimal control surface and hinge moments, there is a design space to be explored relating the LE flap chord to deflection required along the wing span.

It can be generally inferred that the present techniques can be used for optimisation of LE and TE flap geometry. Obviously some experiments at certain key-points will be helpful in "boosting" the confidence level. It is realised that other factors such as Mach number effects also come into play and the techniques will need a certain amount of validation work.

5. SELECTED PREDICTIONS ON EXPOSED WING (CONFIG-A), Mach 0.4

These results have been presented to show the capability for studying Mach number effects. At this stage, however, we do not have any experiments to compare with.

Fig.5.1 shows the results for the basic wing (LEF/TEF: 0/0) for Reynolds number variation (R = 10, 20 and 40 $x10^6$) with LE radius r/c = 0.0022.

Fig.5.2 shows predictions for the configuration without LE, TE flap deflections and vortex breakdown effects.

As might be expected, the predictions are similar in character to those at Mach 0.18. It will be of interest to investigate higher Mach numbers in due course.

6. SELECTED PREDICTIONS ON WING-BODY, CONFIG-B, MACH 0.18

For the configuration depicted in Fig.2.2, preliminary calculations have been undertaken. The main purpose at this stage is to demonstrate that the predictive method continues to give a useful insight into complex configuration flow-fields. We need however, to validate the predicted results against experiments in due course on 0.1 and 0.55 scale models (Section 1.2).

Fig.6.1 shows predictions for the configuration without LE, TE flap deflections and vortex breakdown effects. The coefficients are non-dimensionalised by gross wing area. Several curves using different assumptions including LE radius changes are depicted. Strong lift and drag effects arise when vortex flow terms arising on the fuselage are included. This is in line with conclusions of Ref.5. The induced drag factors are higher than those for the exposed wing (Section 3).

Fig.6.2 shows the effect of LEF/TEF: 45/0 case. The improvements in lift and drag properties of the configuration are clearly shown and the results look plausible. However, these need to be placed in a more complete

perspective and further work with a range of LE and TE flap deflections will be required in due course.

7. SCOPE OF FURTHER WORK REQUIRED

As mentioned in Ref.6, further work exploiting the potential of the method is seen in a number of aspects e.g.:

1. LEF and TEF Shape optimisations. Systematic parametric studies are required. These will allow the design cycle to commence with a good idea of the relative effectiveness of the various controls and the changes needed in the flight control system.

2. Validations with fuselage effects (complete configurations).

3. Pitching moment considerations for trim.

4. Predictions of characteristics of other related planforms: diamond, Y- and Lambda etc.

5. Predictions and Comparisons for the F-16 "Falcon" configuration.

6. Improvements e.g. Relaxed Wake Consideration.

7. Sideslip, operation with different LEF and TEF settings either side to prevent adverse vortex breakdown effects.

8. Assessment of possibilities for further developments including trimming, aero-elastics, transonics.

In view of the encouraging progress and significant problems already solved, the time scales envisaged are likely to be reasonable.

The predictions can guide CFD and experimental work which should lead to considerable cost benefits.

These topics should have a constructive impact on the current and future practical scene.

8. CONCLUDING REMARKS

A topical research area motivated by "stealth" considerations concerns high lift development on aircraft with thin, highly tapered "diamond" planform wings. The main drive is towards improving subsonic and transonic manoeuvrability with LE and TE devices.

This report has addressed **two** main objectives. The **first** objective has been to assess the given "diamond" wing with and without LE and TE flaps. The **second** objective is towards seeking ideas for possible improvements of such wings. The two objectives lead also to the methodology for dealing with such wings when more accurate design information may be required in the future.

The predictive techniques emphasise the first "break" of lift and drag characteristics arising due to Mach and Reynolds number effects. Vortex breakdown effects (second "break") are related directly to the first "break". Delaying the first "break", in general, postpones the second "break". From the point of view of deriving the actual operating schedule for a wing with LE and TE flaps, the vortex breakdown effects become relatively less significant as the LE flap deflection progressively increases or LE radius increases.

The agreement between predictions and experiment for the first break with and without LE radius effects is remarkably encouraging. This once again confirms that theory predicts with reasonable confidence, the LE radius and Reynolds number effects.

It is very encouraging to note that the theoretical predictions of lift-drag envelopes are very close to comparable experimental results. The theory appears capable of predicting the flap schedules, although we have not needed to include all the features of the theory available to us (e.g. relaxed wakes, viscid corrections at the expense of course, of extra complexity). Vortex breakdown effect limits are "pushed" higher by increasing LE flap deflection.

For a wing with scheduled LE and TE flaps, the benefits of rounded LE are apparent at high lift. Increasing Reynolds number (flight conditions) will add to these improvements.

For equivalent lift-drag performance, a sharp LE wing will in general, require a higher LE deflection and the deflection schedule will need to be kept closely "tuned". On the other hand, even small amounts of rounding on the LE allows a much more tolerant deflection schedule.

A brief assessment of LE flap chord showed that a smaller chord LE flap implies reduced effectiveness and to an extent this may be compensated for by increased deflection. The techniques available allow us to assess these benefits.

A brief study with fuselage vortex flows indicated very significant trends which appeared to be plausible. However, these need to be placed in a more complete perspective and further work with a range of LE and TE flap deflections will be required in due course.

Capability is for reliable lift-induced drag prediction through Mach and Reynolds number ranges covering Model or flight. Methods can be used for optimisation studies at the configuration design stage or during wind tunnel testing phase. Applicability is for wide ranging configurations including conventional and unconventional (diamond, lambda-, y- "stealthy" wings).

The methods provide the ability to determine pay-offs arising from geometry changes and device incorporation. With these methods, considerable cost benefits are implicit which can be justified. For example, any "non-promising" configurations on the basis of the predictions need not be tested in full detail, saving costs. The effort can be better expended on tests of more "useful" configurations. Similar arguments apply for CFD.

Such information will lead to an improved appreciation of compromises to be made between constraints imposed by radar signature considerations and aerodynamic performance.

ACKNOWLEDGEMENTS

The author has pleasure in acknowledging helpful technical discussions with Dr. W. Calarese (formerly EOARD, London, UK), Mr. R.F. Osborn, Capt. M. Alexander, Lt. J. Seo. Mr. K. Langan and scientists at USAF-FIMM-WL, Ohio. Thanks are also due to Mr. S. Galpin for technical assistance.

The work reported has been, in part, supported by the USAF-EOARD (SPC-93-4023) and this is gratefully acknowledged.

Lastly it should be mentioned that any opinions expressed are author's own

REFERENCES

1. NANGIA, R.K., "Report on "Window-on-Science" Visit (April 1992), RKN/TP-92-112, 4th May 1992. Copies submitted to USAF-EOARD, London.

2. GALLAWAY, C.R. & OSBORN, R.F., "Aerodynamics Perspective of Super-Maneouverability", AIAA-85-4068, 1985.

3. NANGIA, R.K., "Outline Technical Proposal, High Lift Wing Development Programme on Typical Modern & Future Combat Aircraft Configurations", RKN/TP-92-114, 24th June 1992.

4. LAN, C.E. & HSU, C.H., "Effects of Vortex Breakdown on Longitudinal and Lateral Aerodynamics of Slender Wings by the Suction Analogy", AIAA Paper 82-1385, August 1982.

5. ERICKSON, G.E. & BRANDON, J.M., "On the Non-linear Aerodynamic and Stability Characteristics of a Generic Chine-Forebody Slender-Wing Fighter Configuration", AIAA Paper 87-2617, 1987.

6. NANGIA, R.K., "Outline Technical Proposal, Areas of Further Work", RKN/TP-93-112, 11th May 1993.

LIST OF SYMBOLS

A	Aspect Ratio
A	Axial Force along x-axis (for definition of C_A)
c	Local Wing chord (function of spanwise position)
c_{aero}	= c, Aerodynamic wing chord
c_{av}	= c, Average Wing Chord
C_A	= A/(q S), Axial Force Coefficient = $C_D \cos\alpha - C_L \sin\alpha$
C_{Ai}	= Axial Force Coefficient without C_{D0} effect
C_D	= D /(q S), Drag Coefficient where D is Drag force
C_{D0}	Drag Coefficient at zero lift (strictly, for a planar wing)
C_{Di}	Lift Induced Drag Coefficient
C_L	= L/(q S), Lift Coefficient, where L is Lift Force
C_{L0}	Lift Coefficient at zero lift
C_{Lmax}	Maximum Lift Coefficient
C_m	= m/(q S c), Pitching Moment (Body Axis)
C_N	Normal Force Coefficient = $C_L \cos\alpha + C_D \sin\alpha$
c_r & c_t	Wing Root chord and Tip chord respectively
k	= π A $C_{Di}/C_L 2$, Lift Induced Drag Factor
LE	Leading Edge
LEF	Leading Edge Flap
m	Pitching moment (Body Axis)
M	Mach Number
q	= 0.5 ρV^2, Dynamic Pressure
r	Aerofoil radius
r_n	Aerofoil radius normal to leading edge of wing
R	Reynolds Number, based on c_{av} (unless otherwise stated)
s	Wing semi-span
S	Wing Area
t	Aerofoil thickness
TE	Trailing Edge
TEF	Trailing Edge Flap
V	Velocity
x,y,z	Orthogonal Wing Co-ordinates, x along bodyaxis
α	Angle of Attack
λ	Taper Ratio
Λ	LE Sweep Angle
η	= y/s, Non-dimensional spanwise Distance
ρ	Air Density

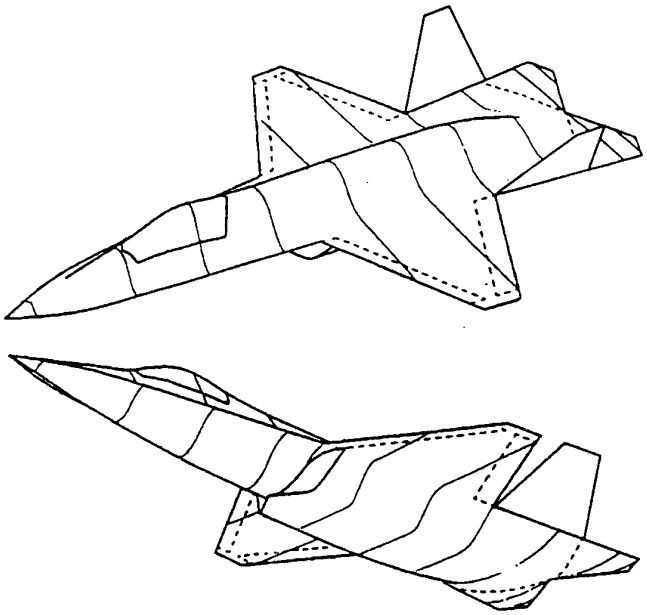

FIG. 1.1 GENERIC AIRCRAFT CONFIGURATION WITH "DIAMOND" PLANFORM WING

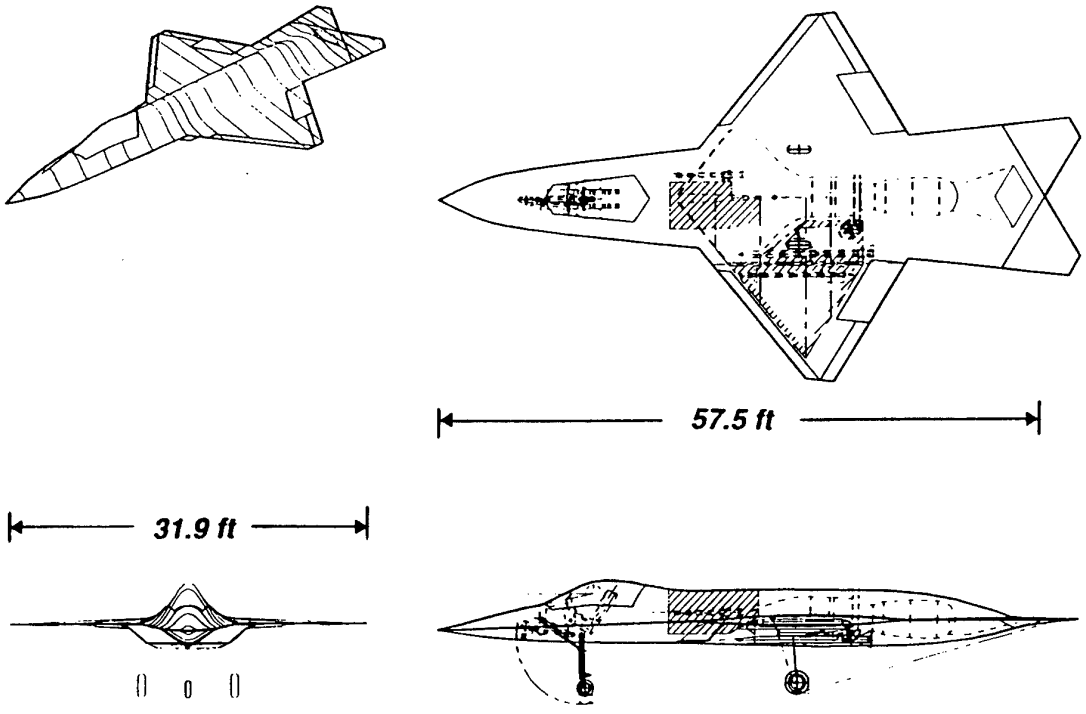

FIG. 1.2 THREE VIEWS OF GENERIC AIRCRAFT

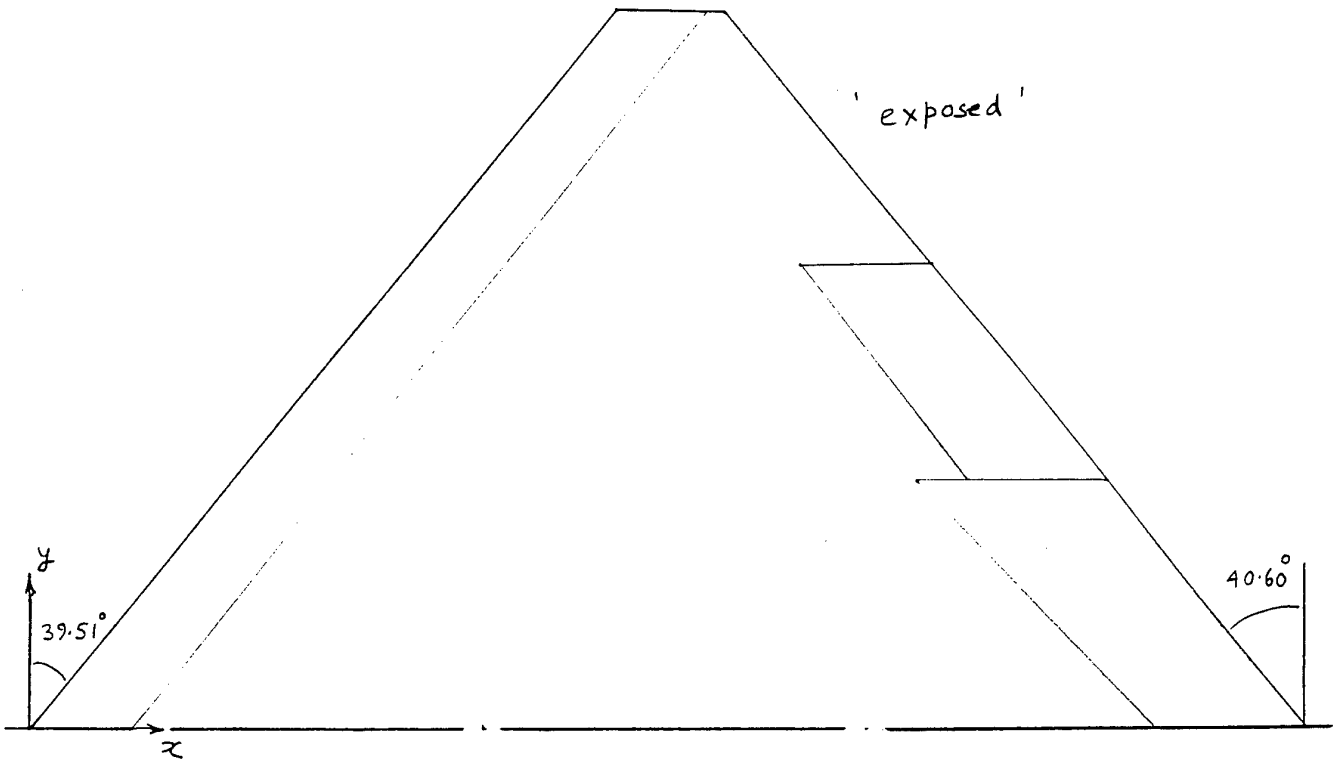

FIG. 2.1 CONFIG-A, WING GEOMETRY, LE FLAP & TE FLAP DETAILS

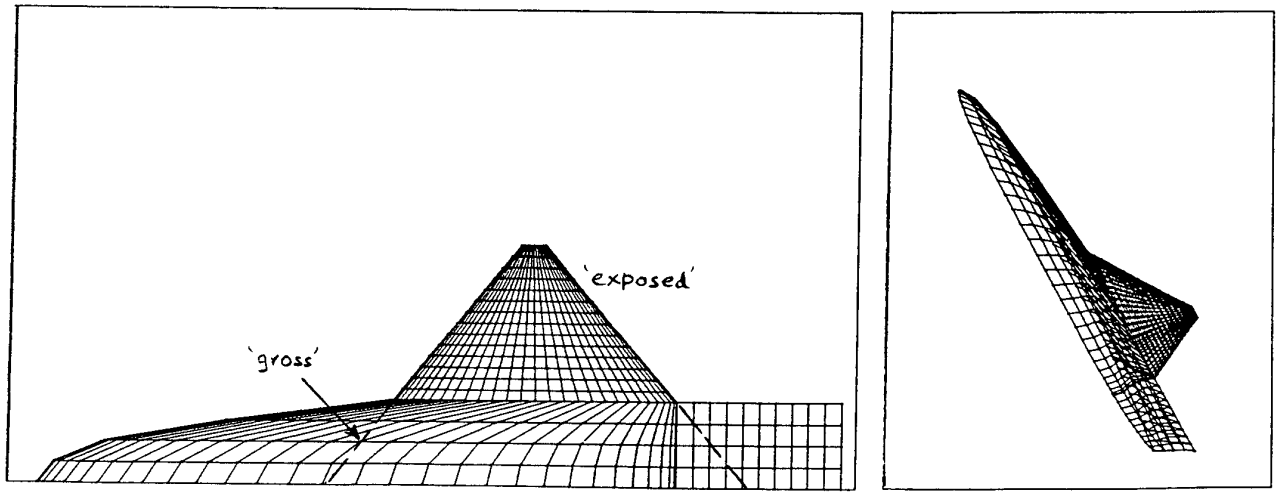

FIG. 2.2 CONFIG-B, GEOMETRY ADOPTED FOR CALCULATIONS

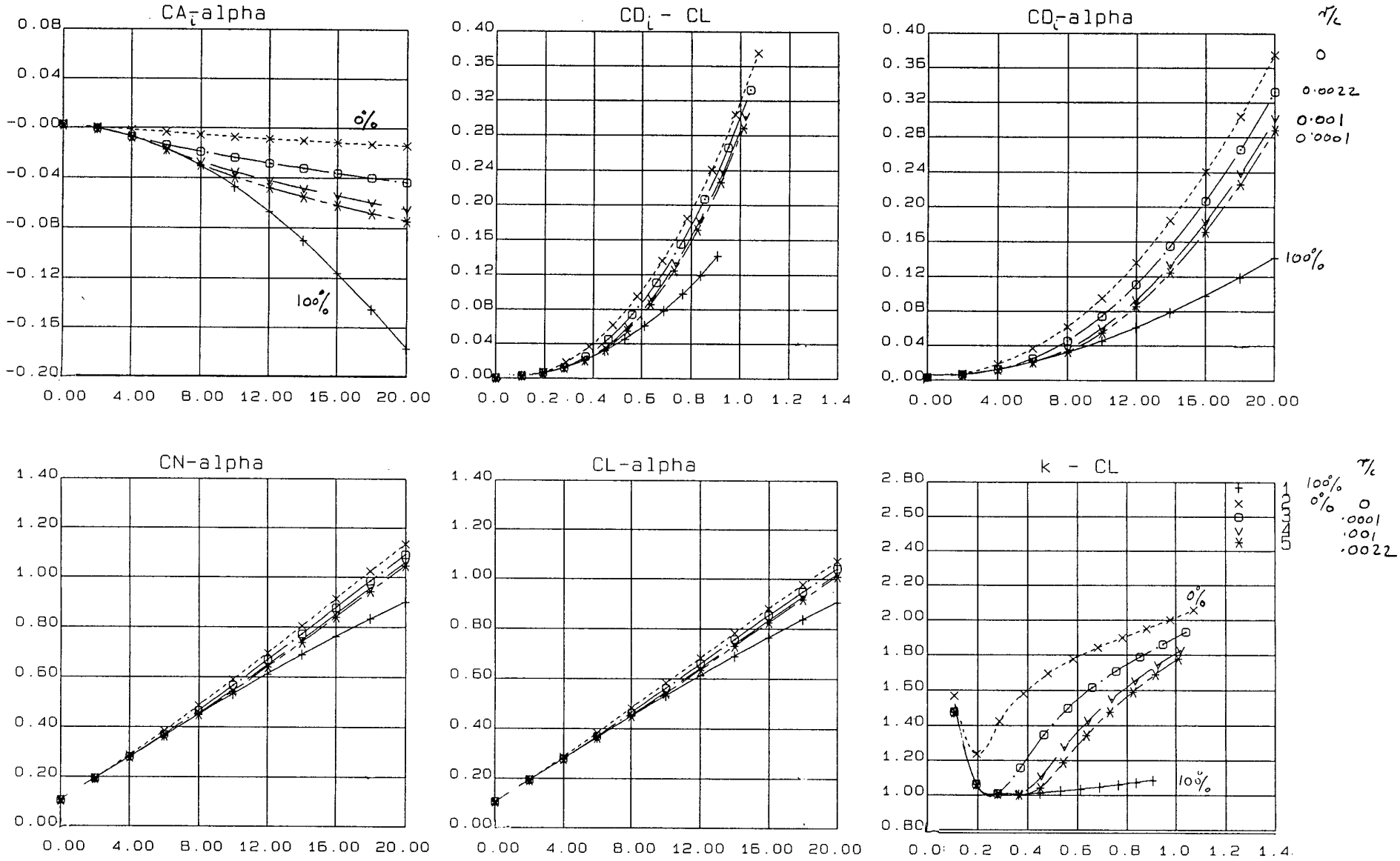

FIG. 3.1 BASIC WING, LE & TE FLAPS UNDEFLECTED, EFFECT OF LE RADIUS VARIATION, MACH 0.18, R = 2 x10^6

PE 1B

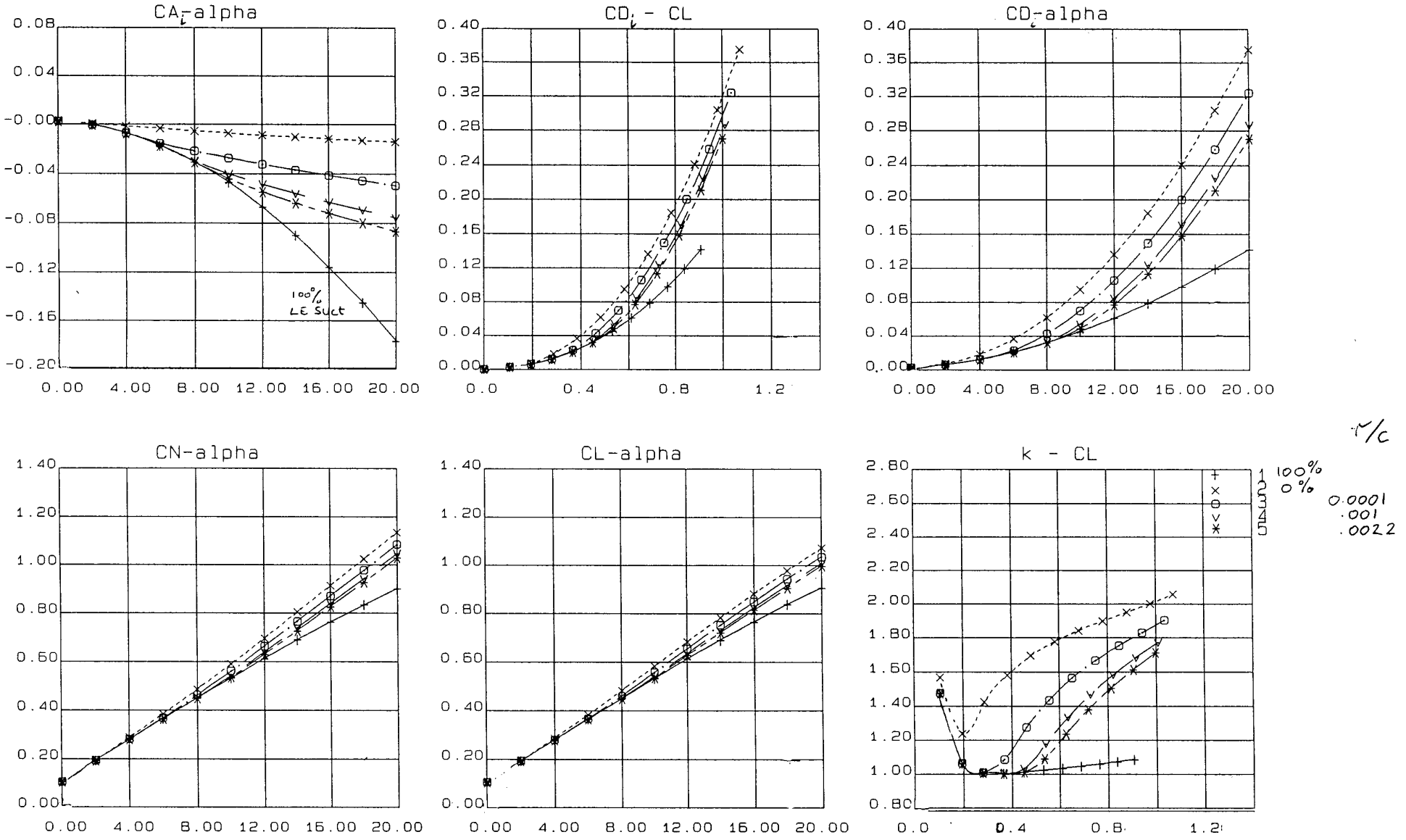

T/C

FIG. 3.2 BASIC WING, LE & TE FLAPS UNDEFLECTED, EFFECT OF LE RADIUS VARIATION, MACH 0.18, R = 5 x10^6

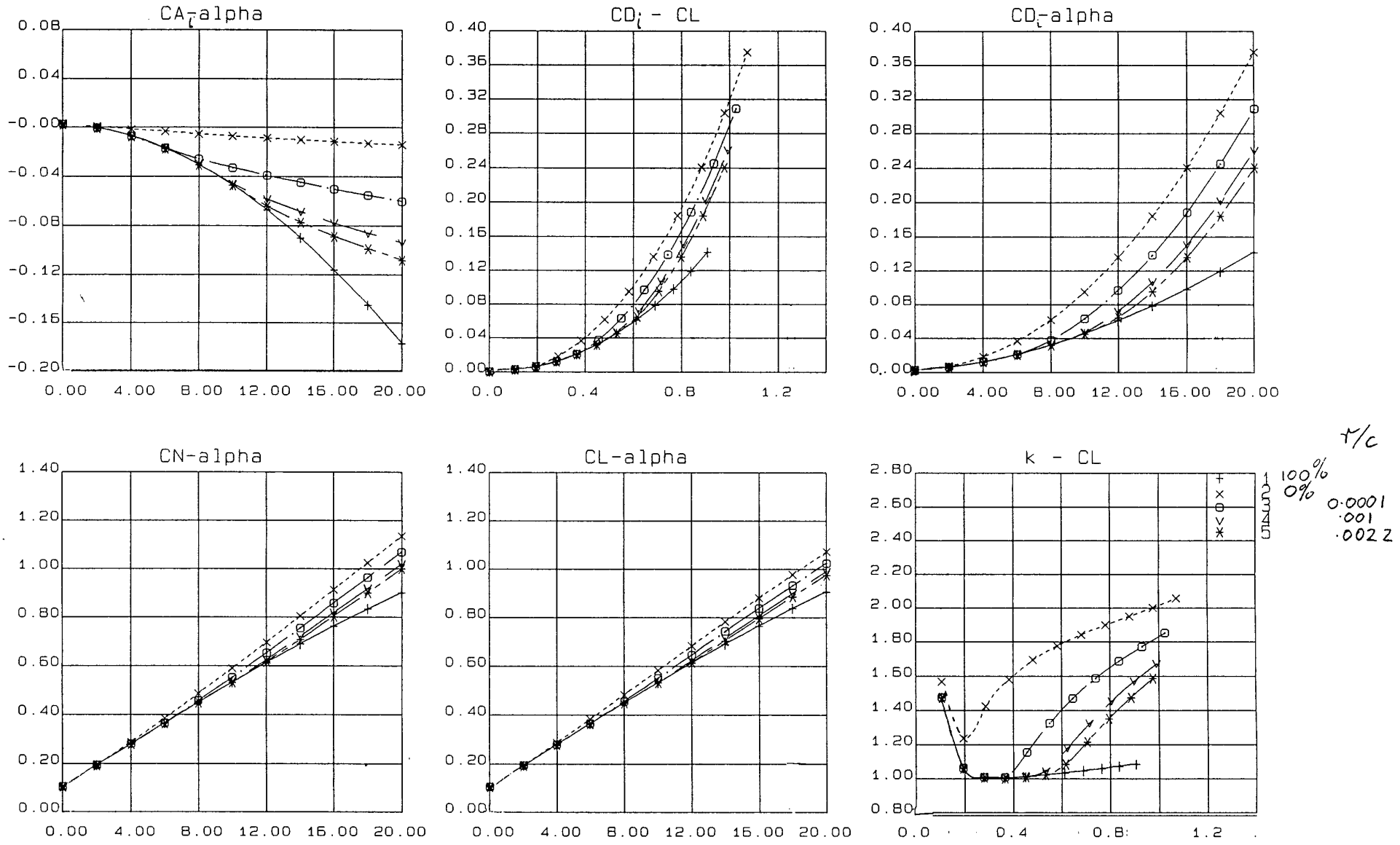

FIG. 3.3 BASIC WING, LE & TE FLAPS UNDEFLECTED, EFFECT OF LE RADIUS VARIATION, MACH 0.18, R = 20 x10^6

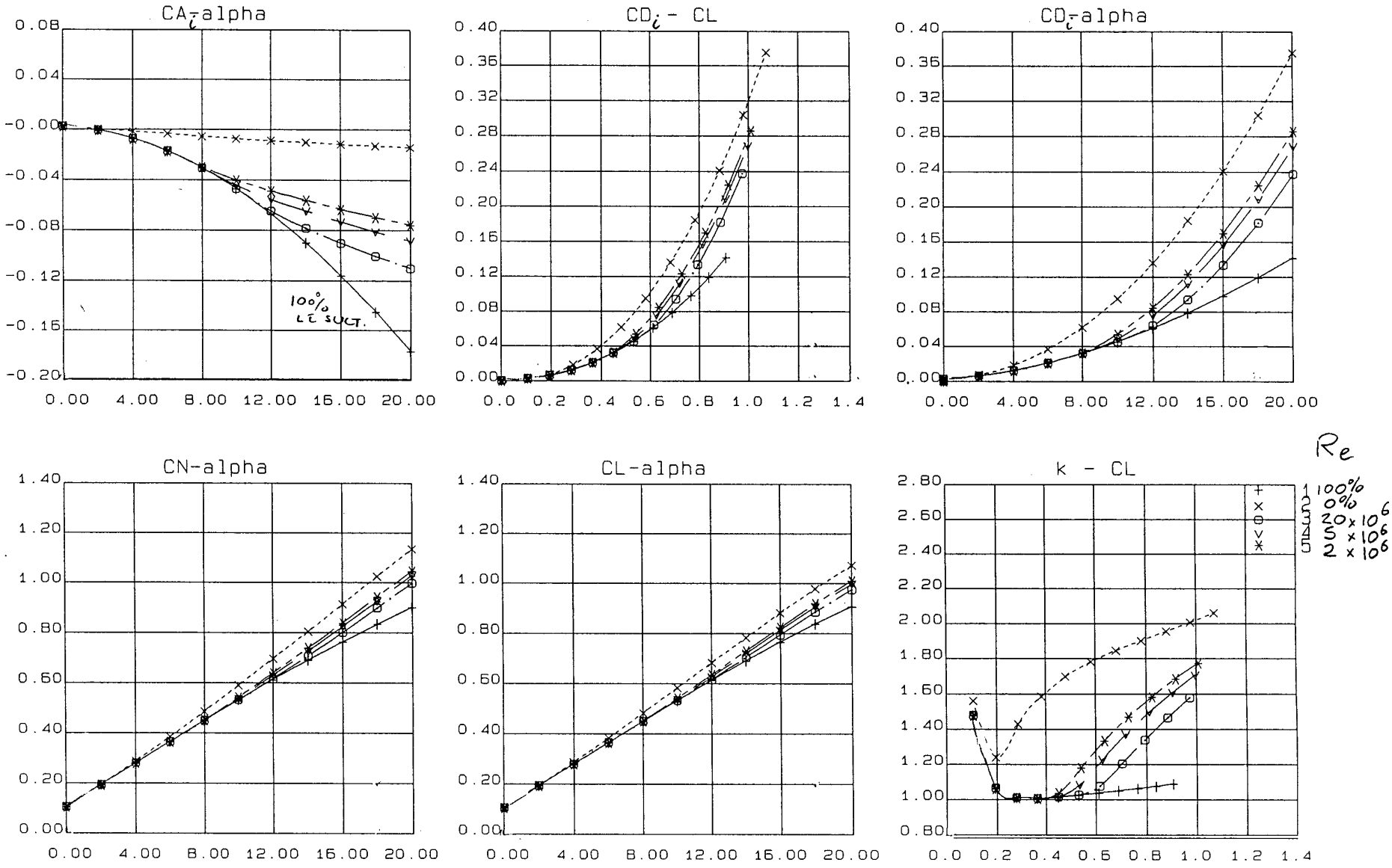

FIG. 3.4 BASIC WING, LE & TE FLAPS UNDEFLECTED, EFFECT OF R VARIATION, MACH 0.18, r/c = 0.0022

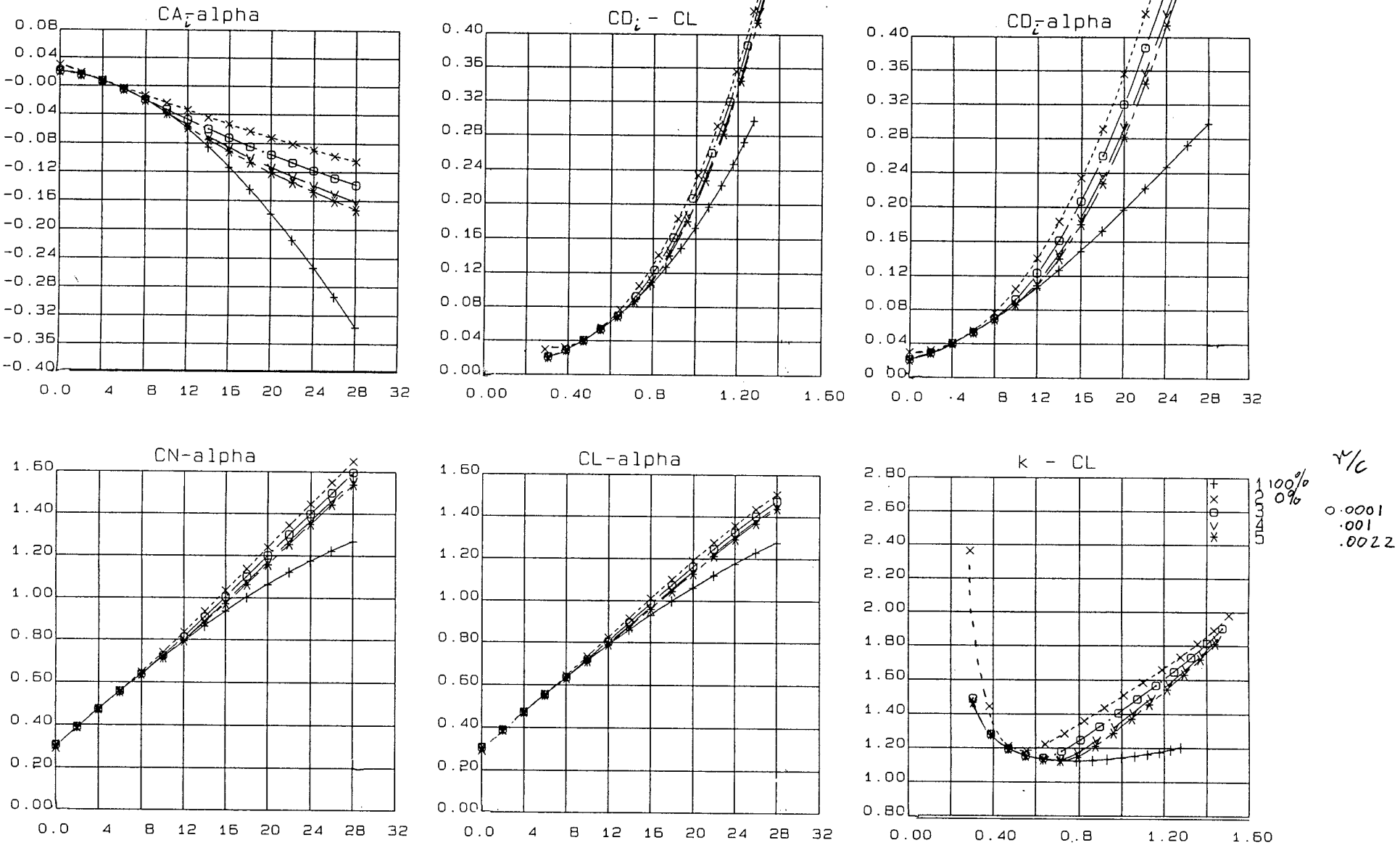

FIG. 3.5 BASIC WING, LEF 15° & TEF 15°, EFFECT OF LE RADIUS VARIATION, MACH 0.18, R = 2 x10^6

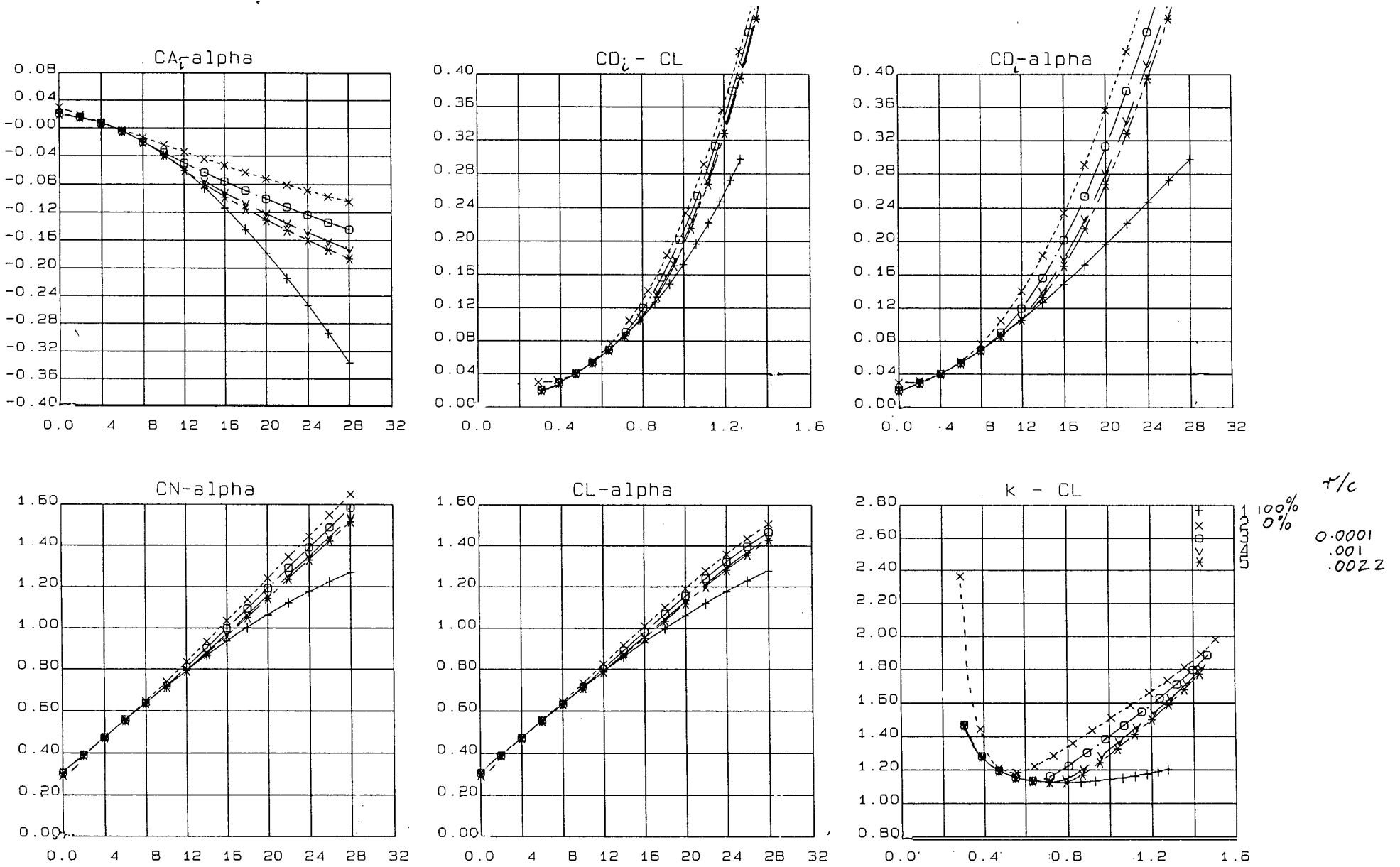

FIG. 3.6 BASIC WING, LEF 15° & TEF 15°, EFFECT OF LE RADIUS VARIATION, MACH 0.18, R = 5 x10^6

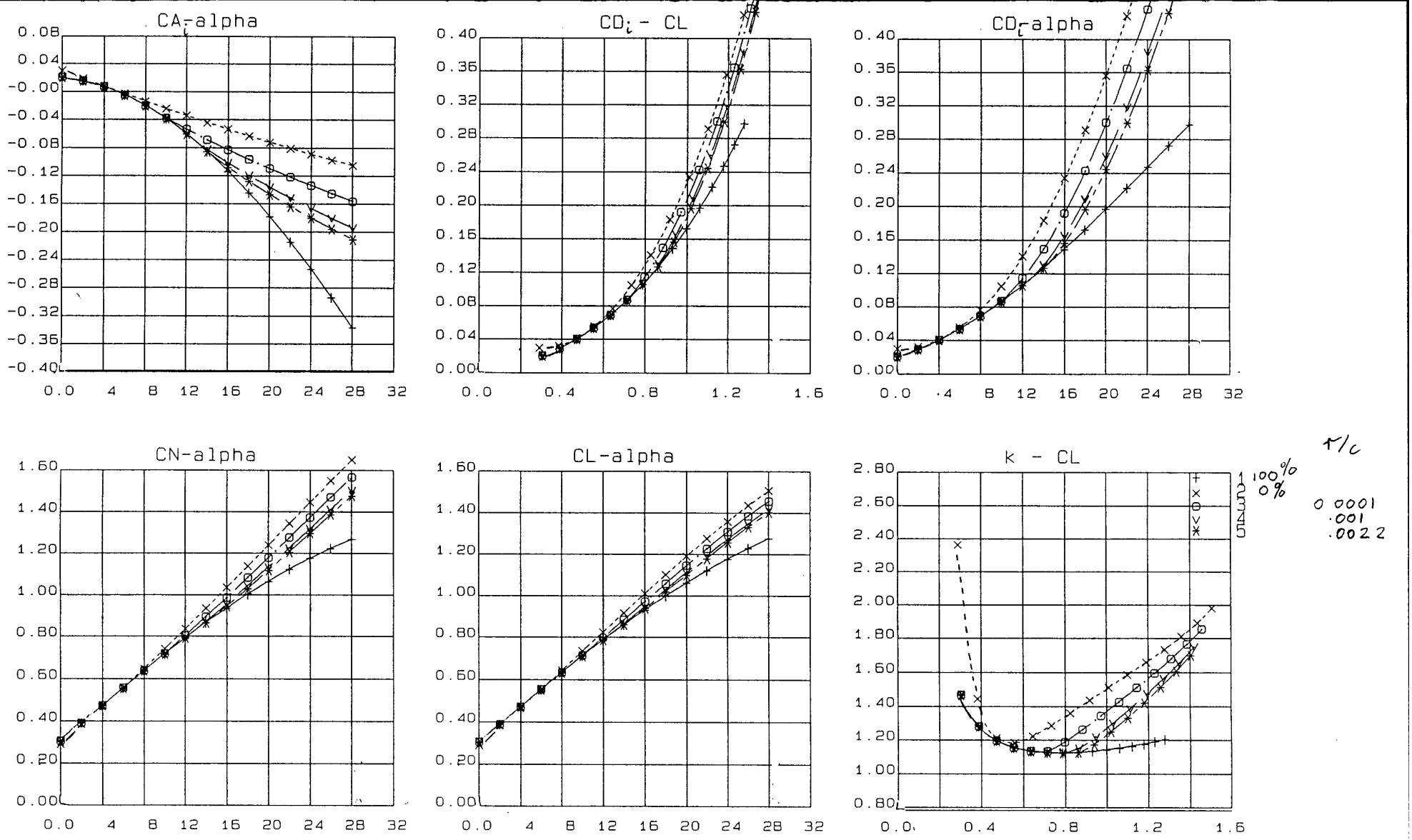

FIG. 3.7 BASIC WING, LEF 15° & TEF 15°, EFFECT OF LE RADIUS VARIATION, MACH 0.18, R = 20 x10^6

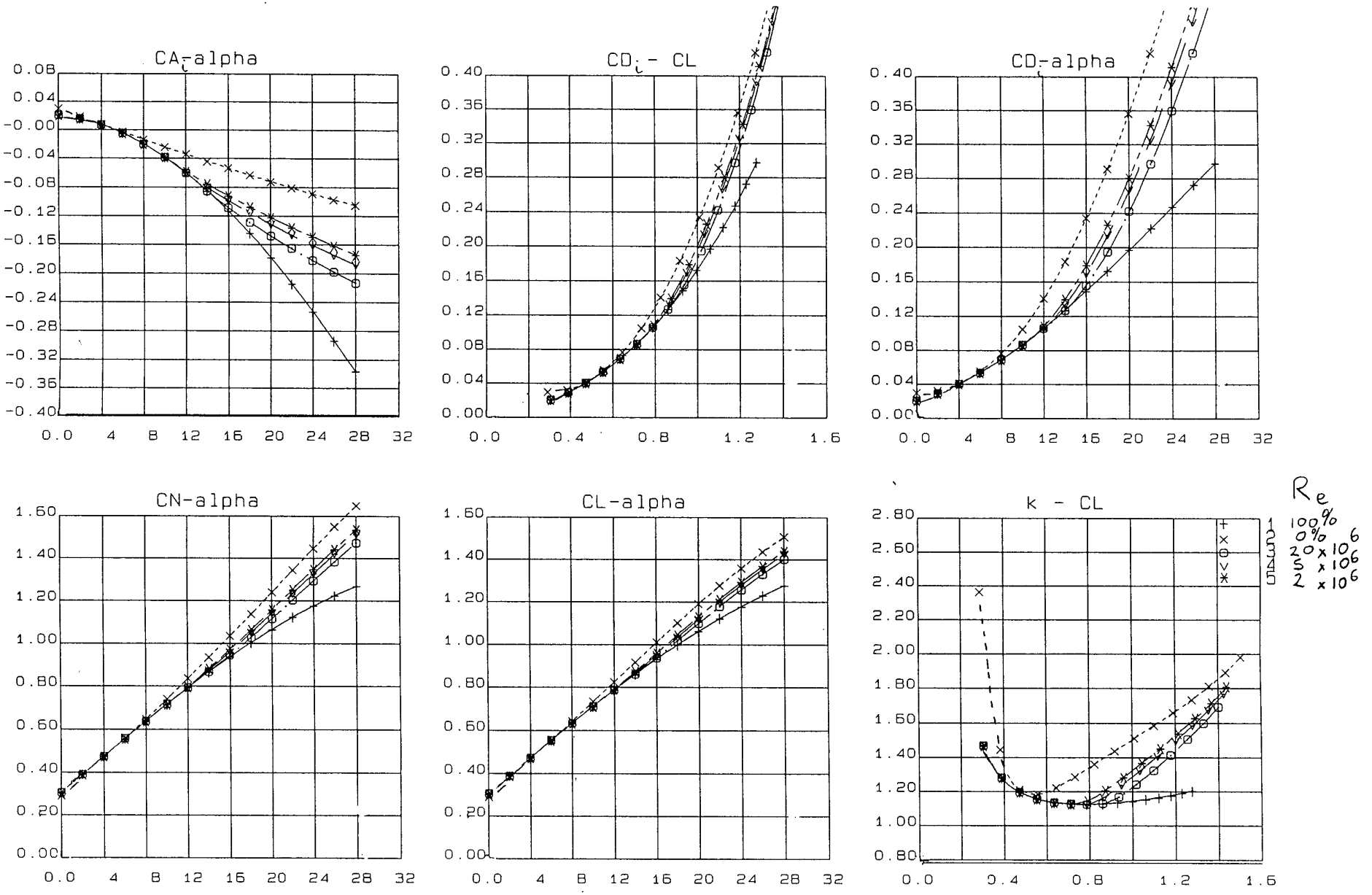

FIG. 3.8 BASIC WING, LEF 15° & TEF 15°, EFFECT OF R VARIATION, MACH 0.18, r/c = 0.0022

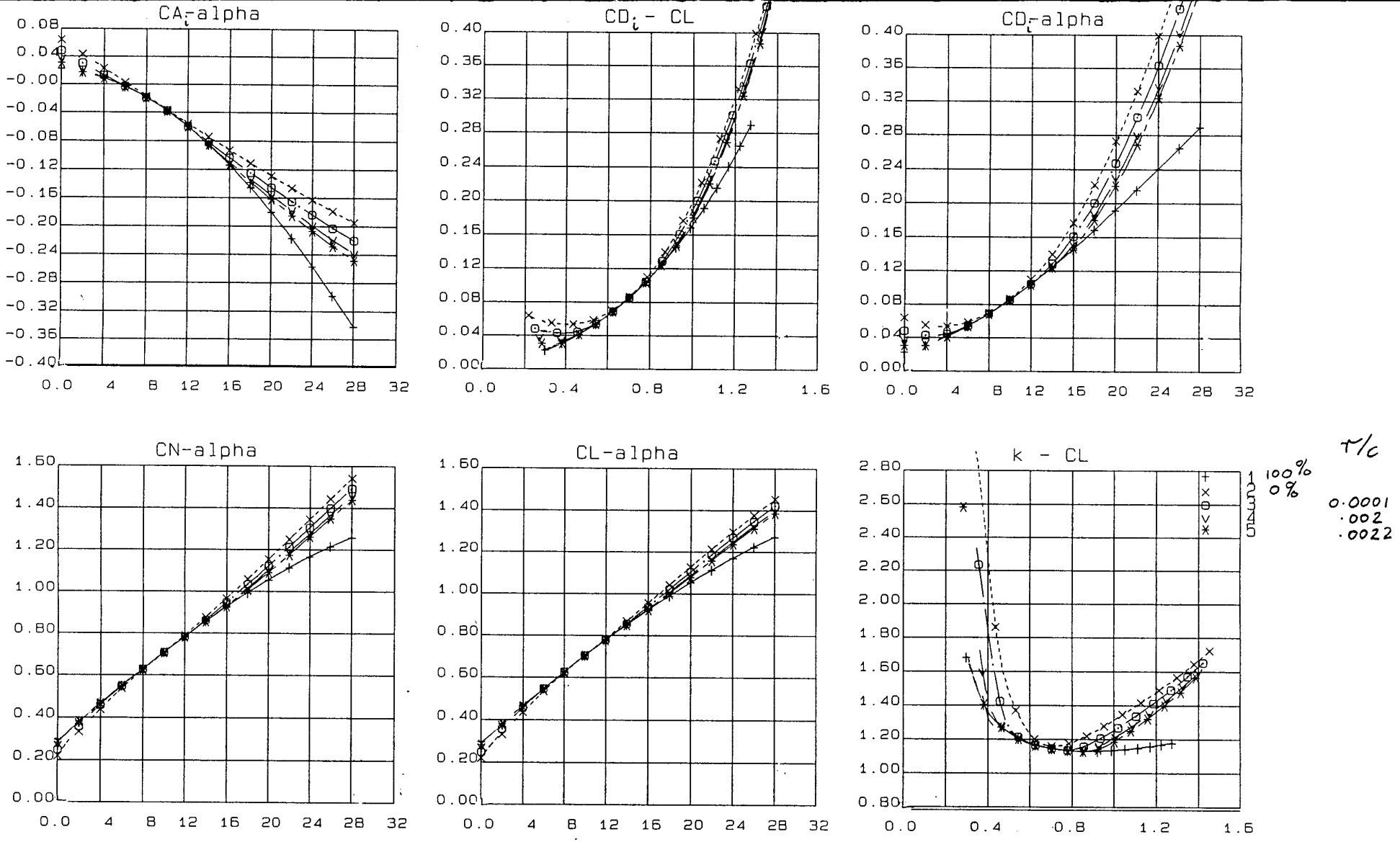

FIG. 3.9 BASIC WING, LEF 30° & TEF 15°, EFFECT OF LE RADIUS VARIATION, MACH 0.18, R = 2 x10^6

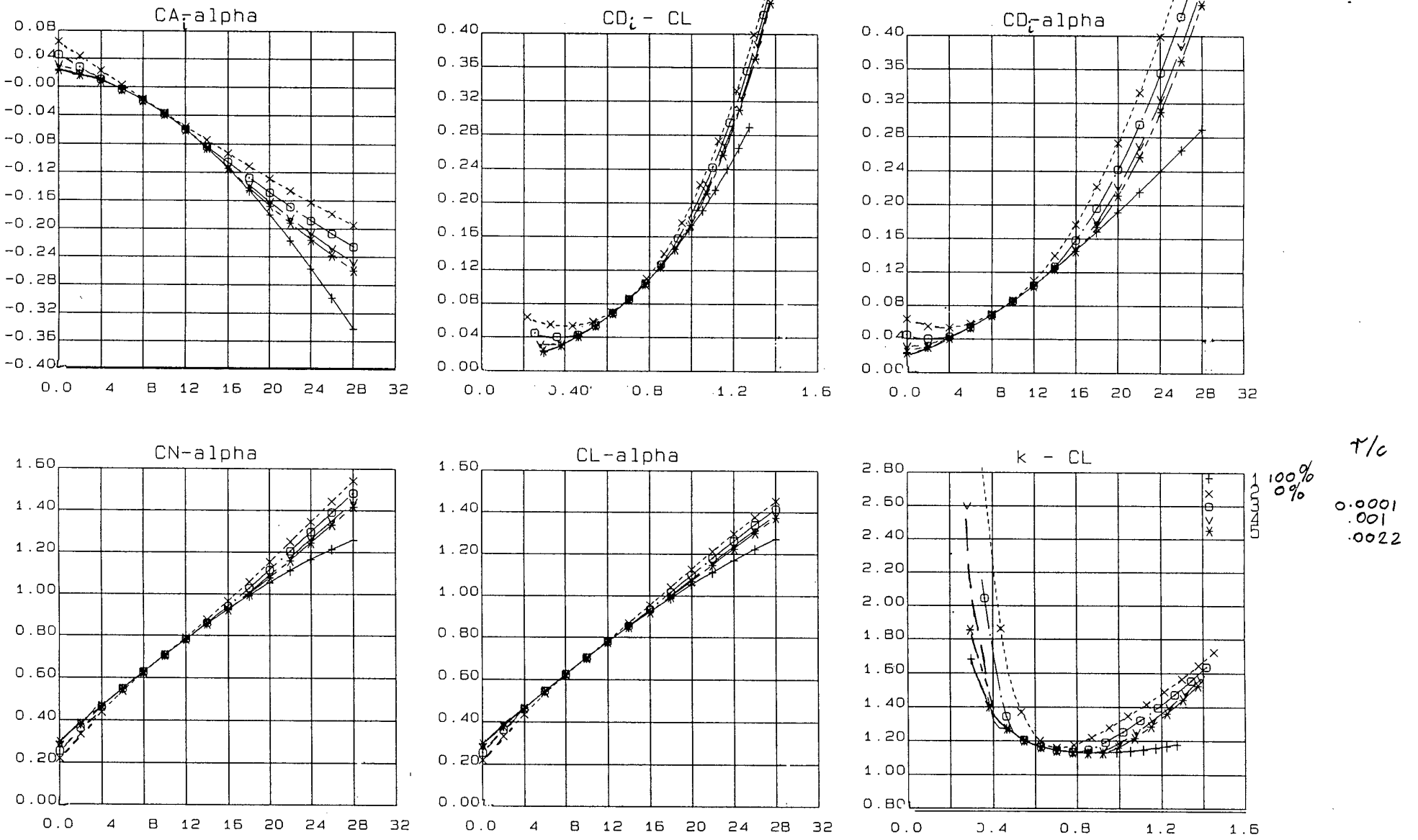

FIG. 3.10 BASIC WING, LEF 30° & TEF 15°, EFFECT OF LE RADIUS VARIATION, MACH 0.18, R = 5 x10⁶

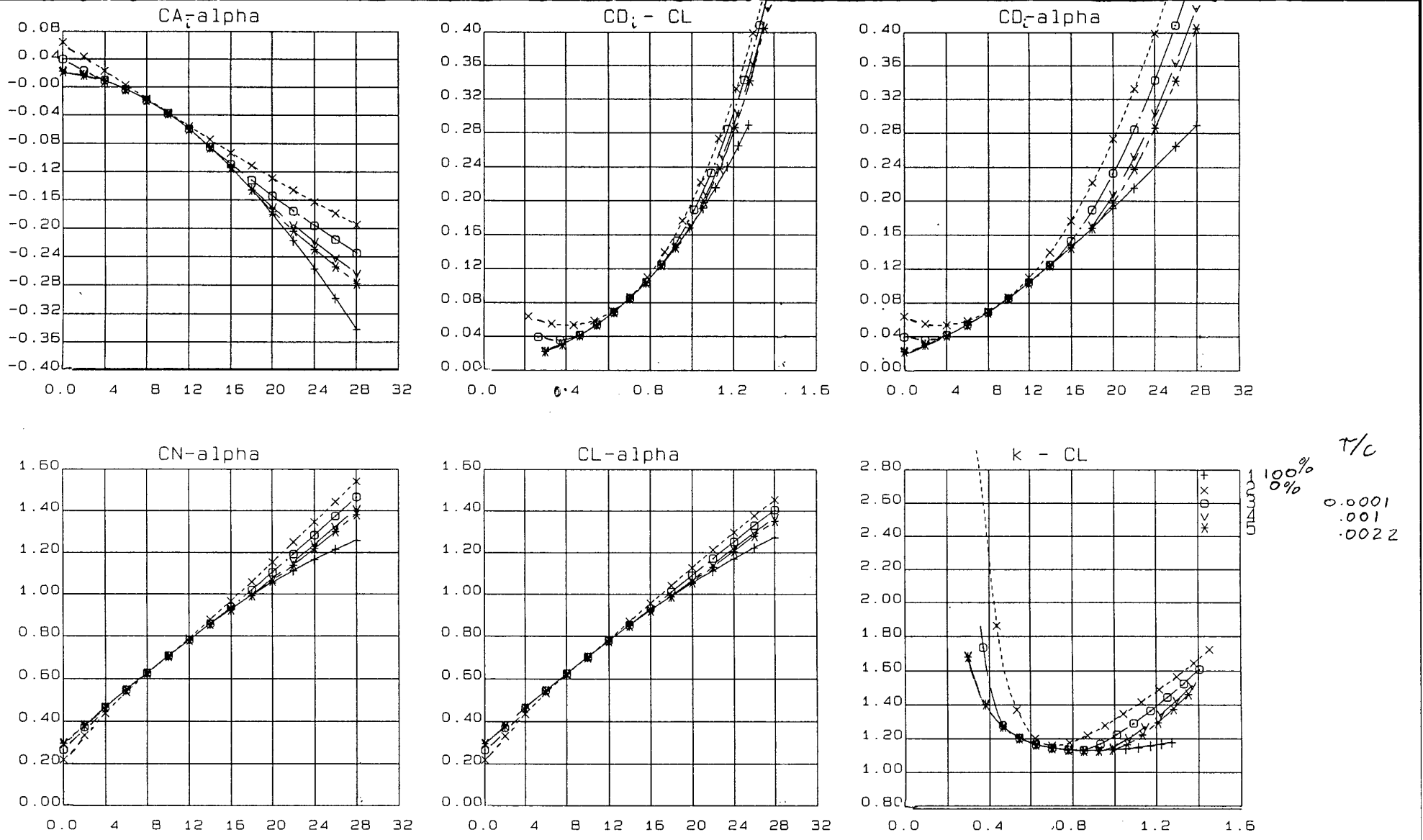

FIG. 3.11 BASIC WING, LEF 30° & TEF 15°, EFFECT OF LE RADIUS VARIATION, MACH 0.18, R = 20 x10^6

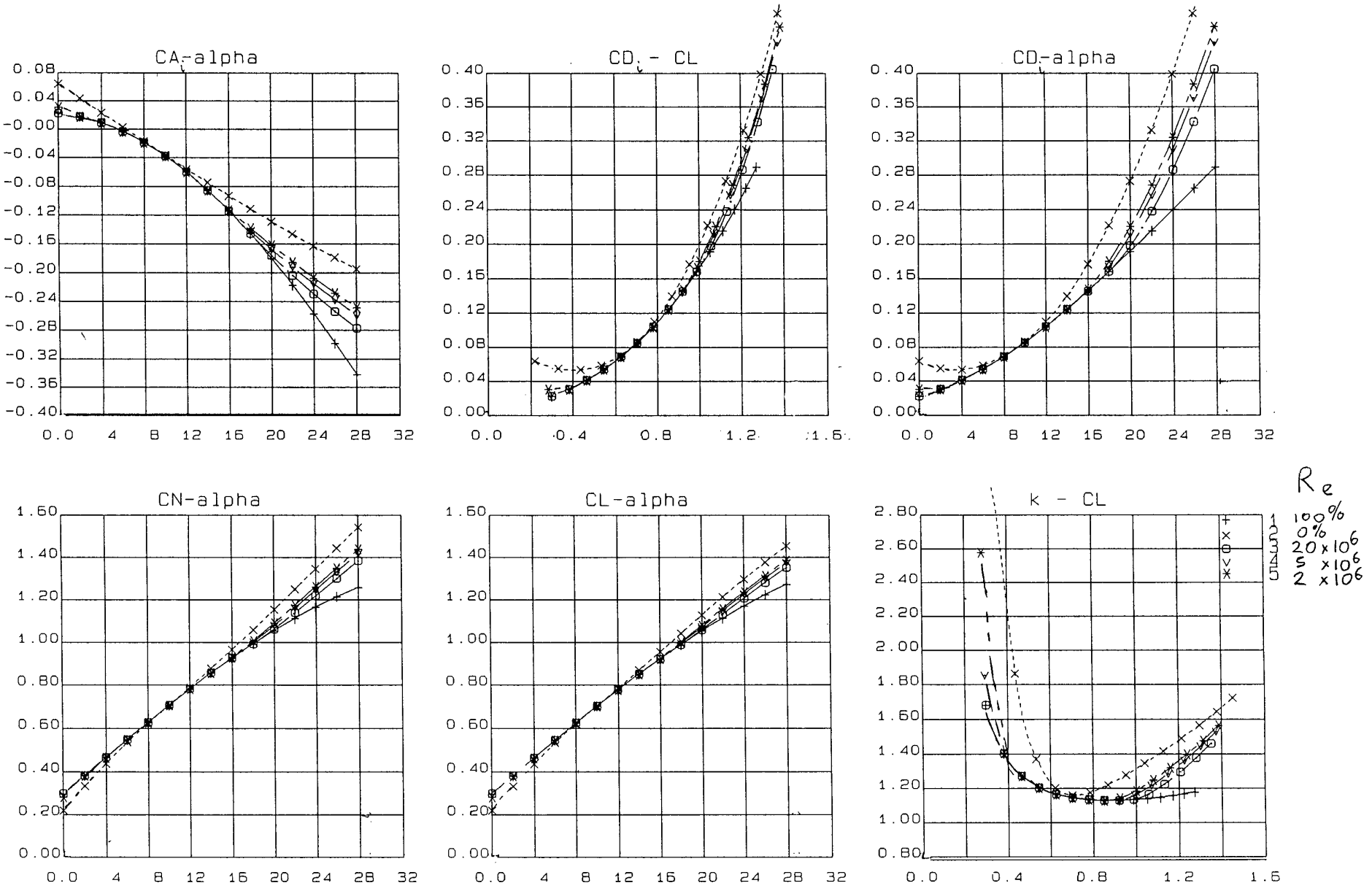

FIG. 3.12 BASIC WING, LEF 30° & TEF 15°, EFFECT OF R VARIATION, MACH 0.18, r/c = 0.0022

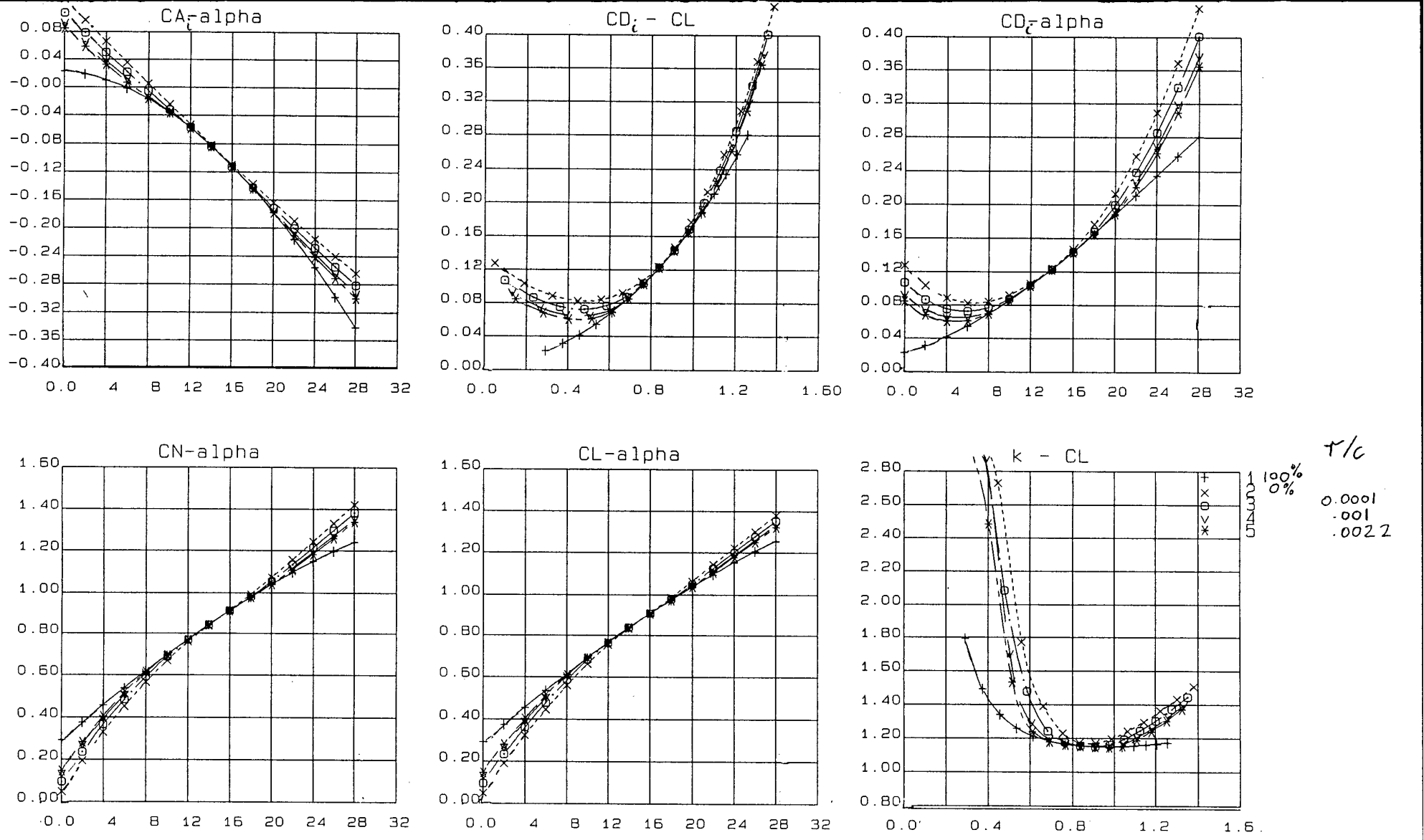

FIG. 3.13 BASIC WING, LEF 45° & TEF 15°, EFFECT OF LE RADIUS VARIATION, MACH 0.18, R = 2 x10^6

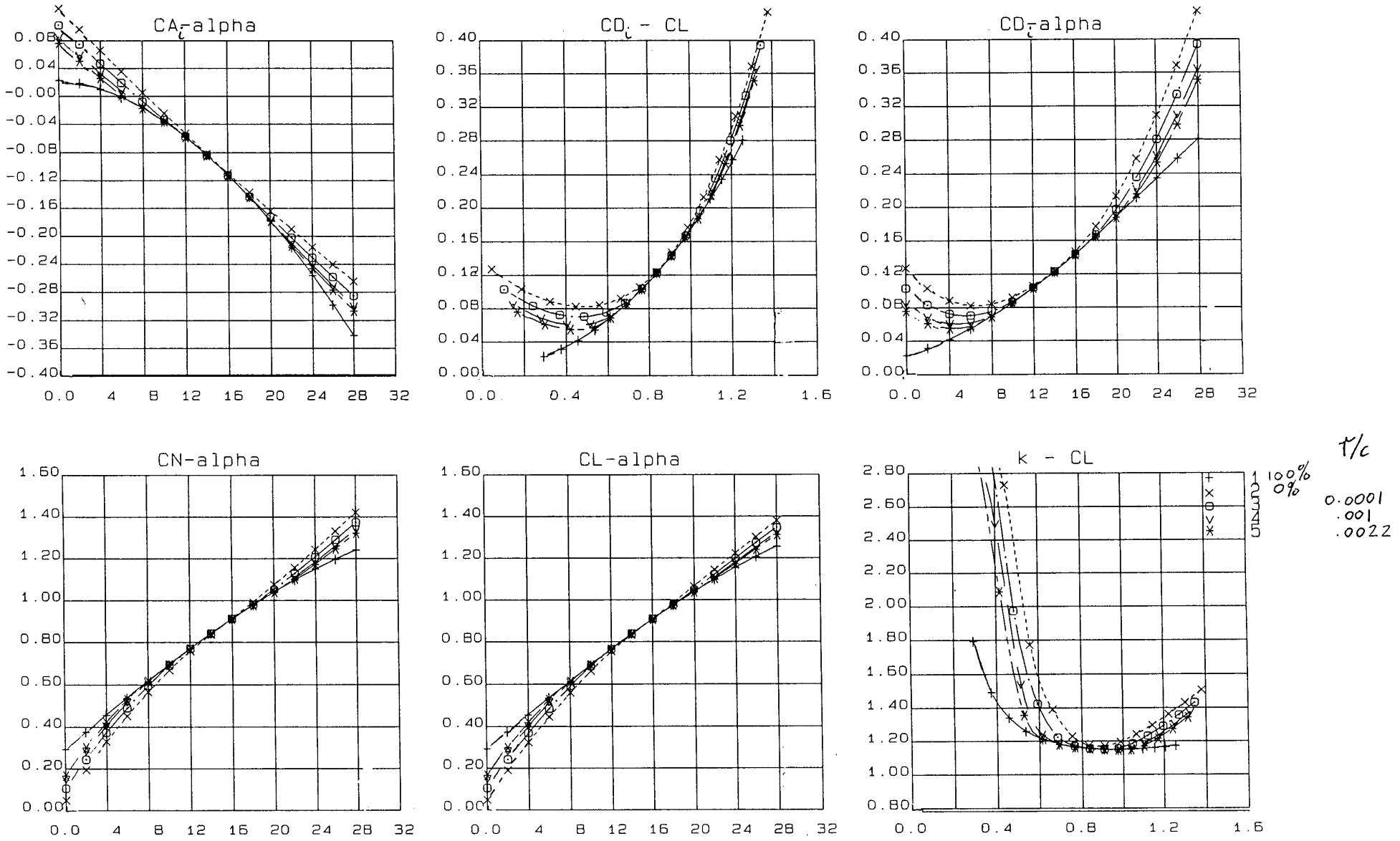

FIG. 3.14 BASIC WING, LEF 45° & TEF 15°, EFFECT OF LE RADIUS VARIATION, MACH 0.18, R = 5 x10^6

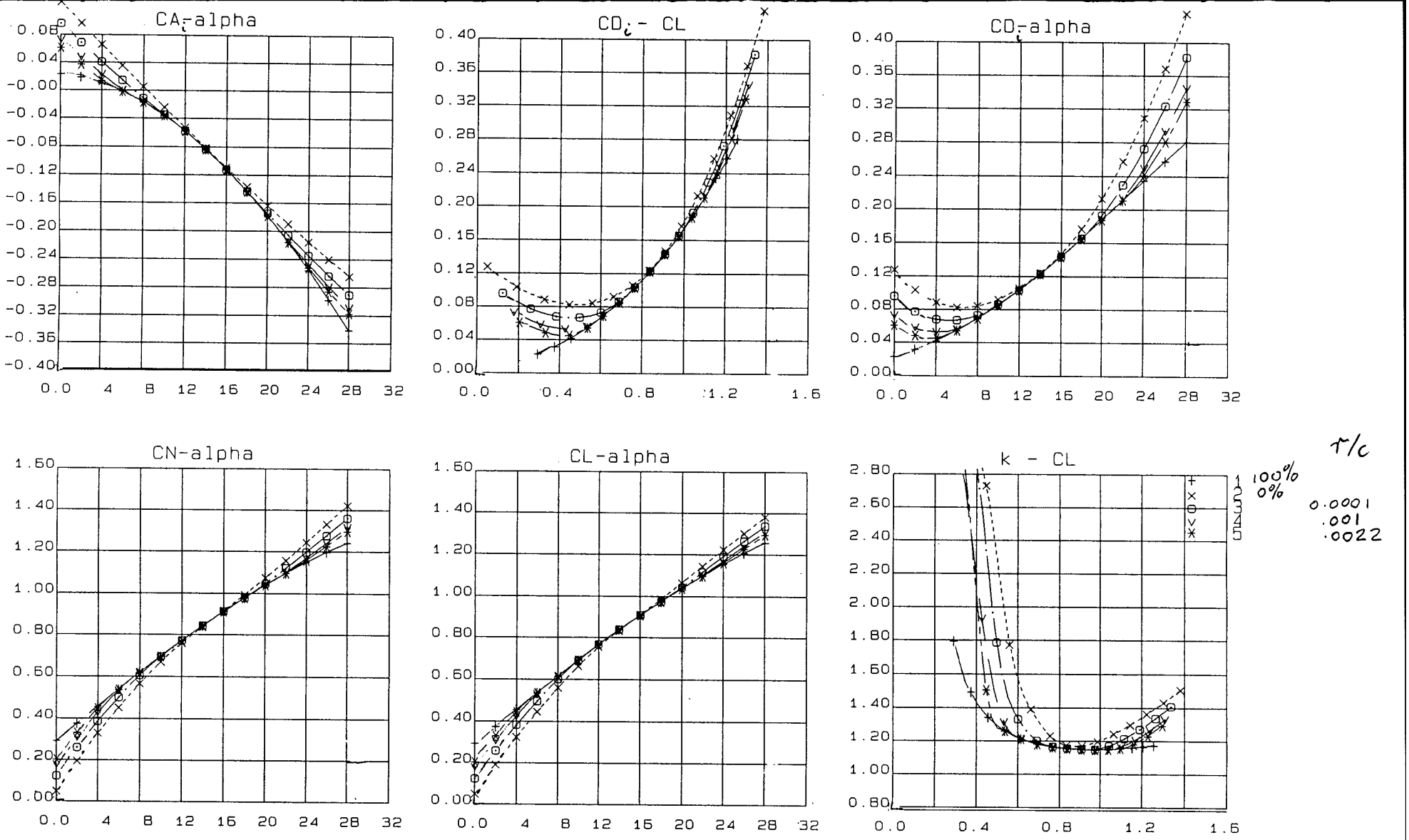

FIG. 3.15 BASIC WING, LEF 45° & TEF 15°, EFFECT OF LE RADIUS VARIATION, MACH 0.18, R = 20 x10^6

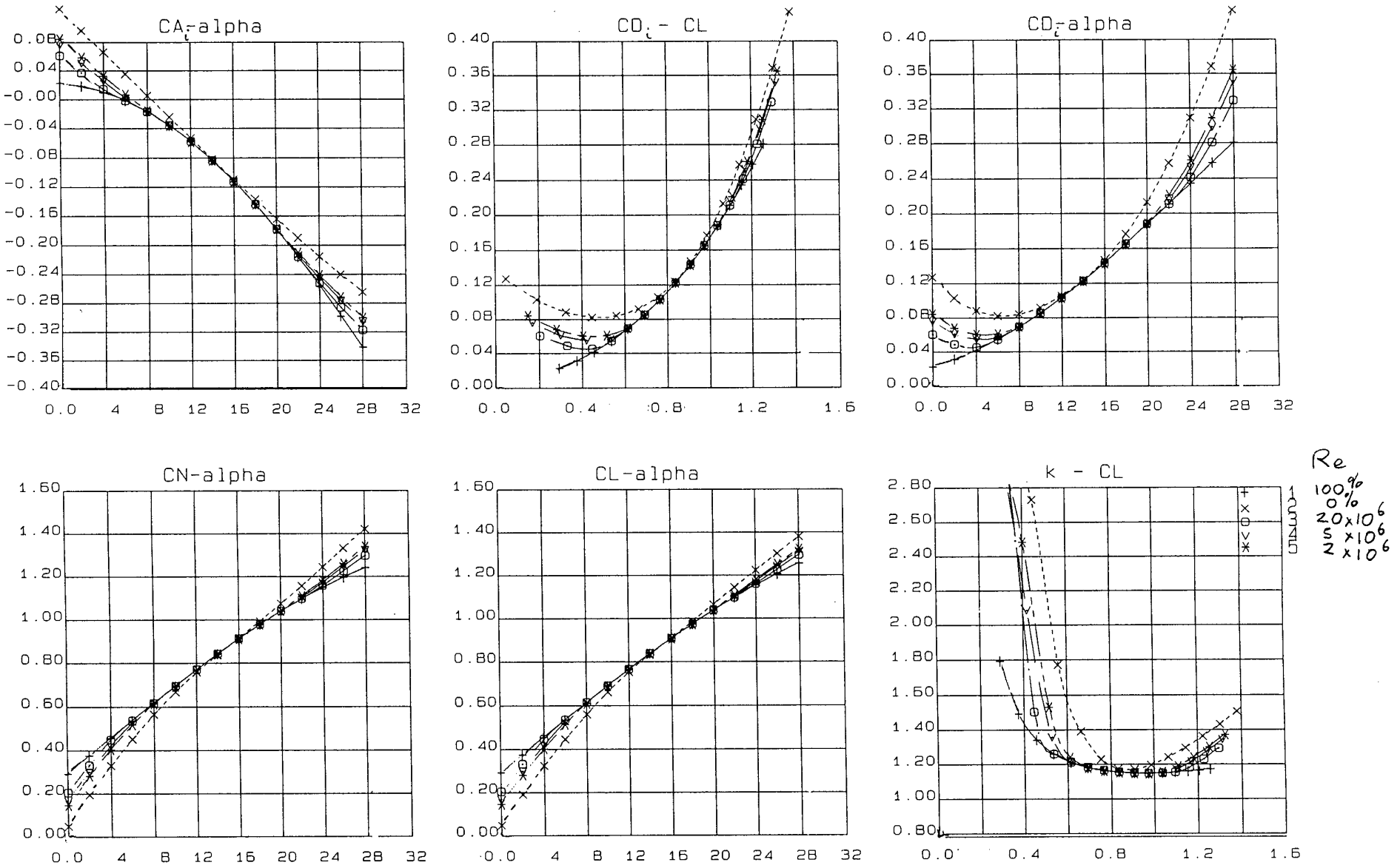

FIG. 3.16 BASIC WING, LEF 45° & TEF 15°, EFFECT OF R VARIATION, MACH 0.18, r/c = 0.0022

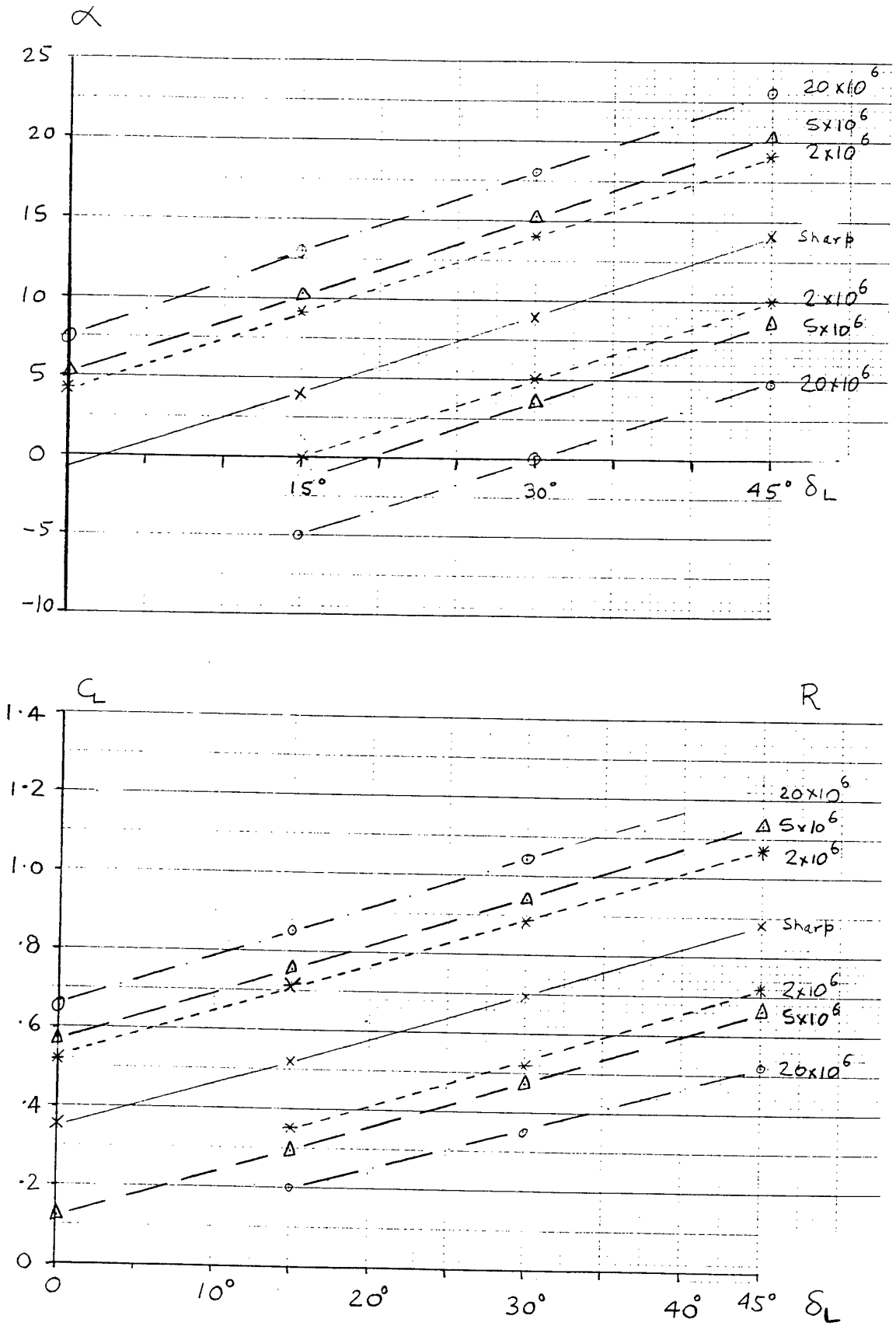

FIG. 3.17 BASIC WING WITH LEF DEFLECTION, TEF 15°, ATTACHED FLOW DOMAINS, α & C_L BASIS, EFFECT OF R VARIATION, MACH 0.18, r/c = 0.0022

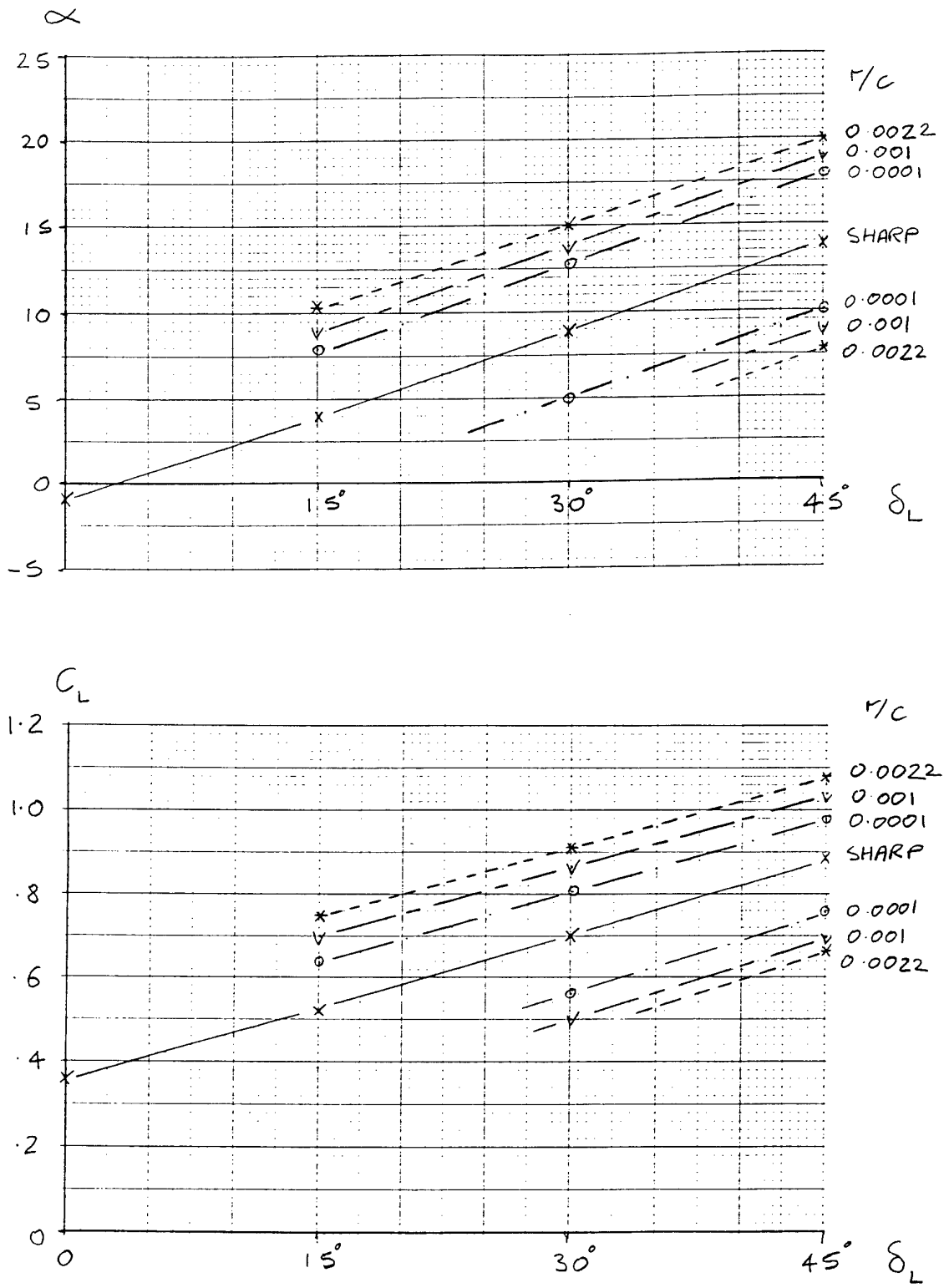

FIG. 3.18 BASIC WING WITH LEF DEFLECTION, TEF 15°, ATTACHED FLOW DOMAINS, α & C_L BASIS, EFFECT OF LE RADIUS VARIATION, MACH 0.18, R = 2, 5 & 20 x10^6

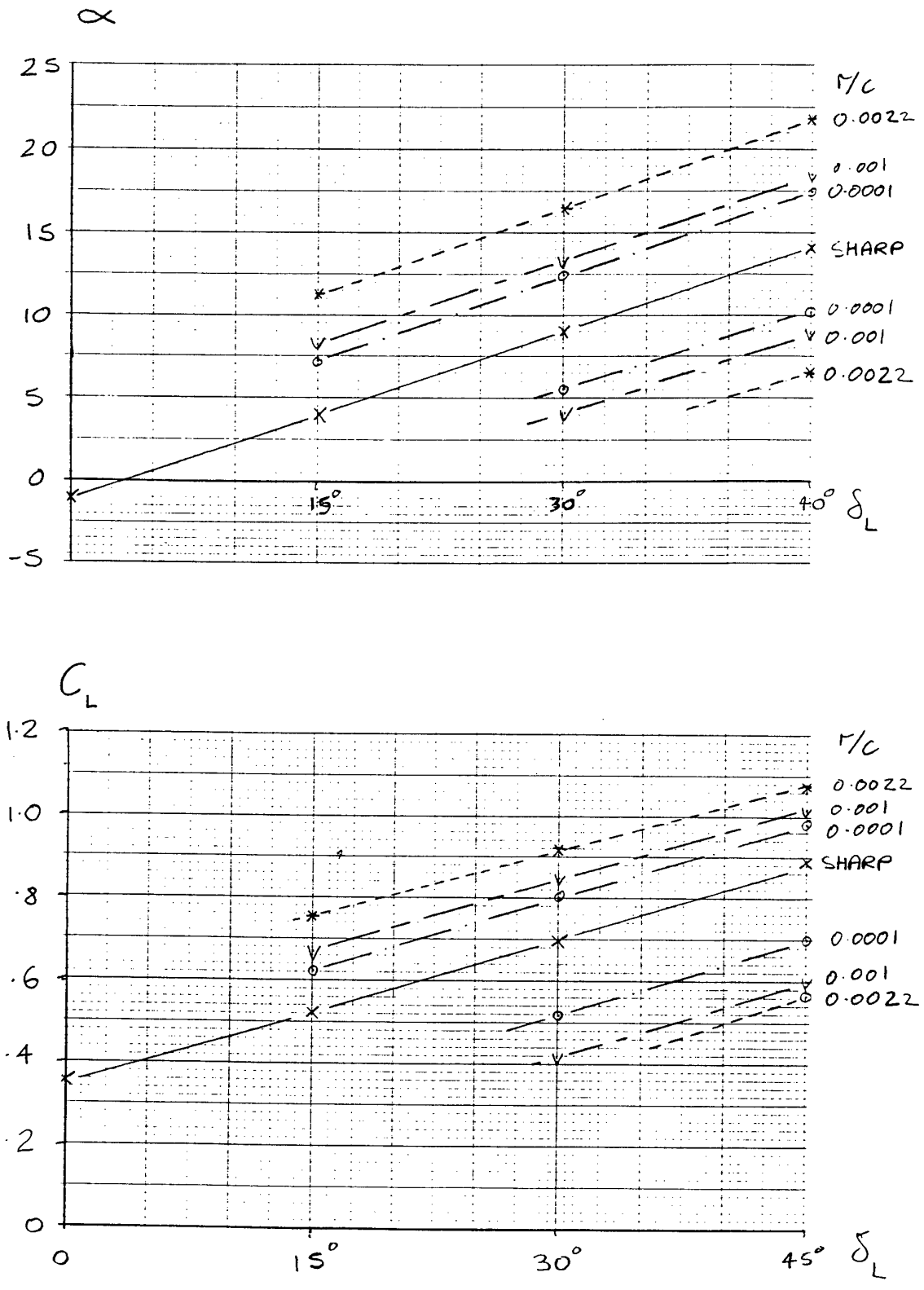

FIG. 3.18 (Cont'd) (b) $R = 5 \times 10^6$

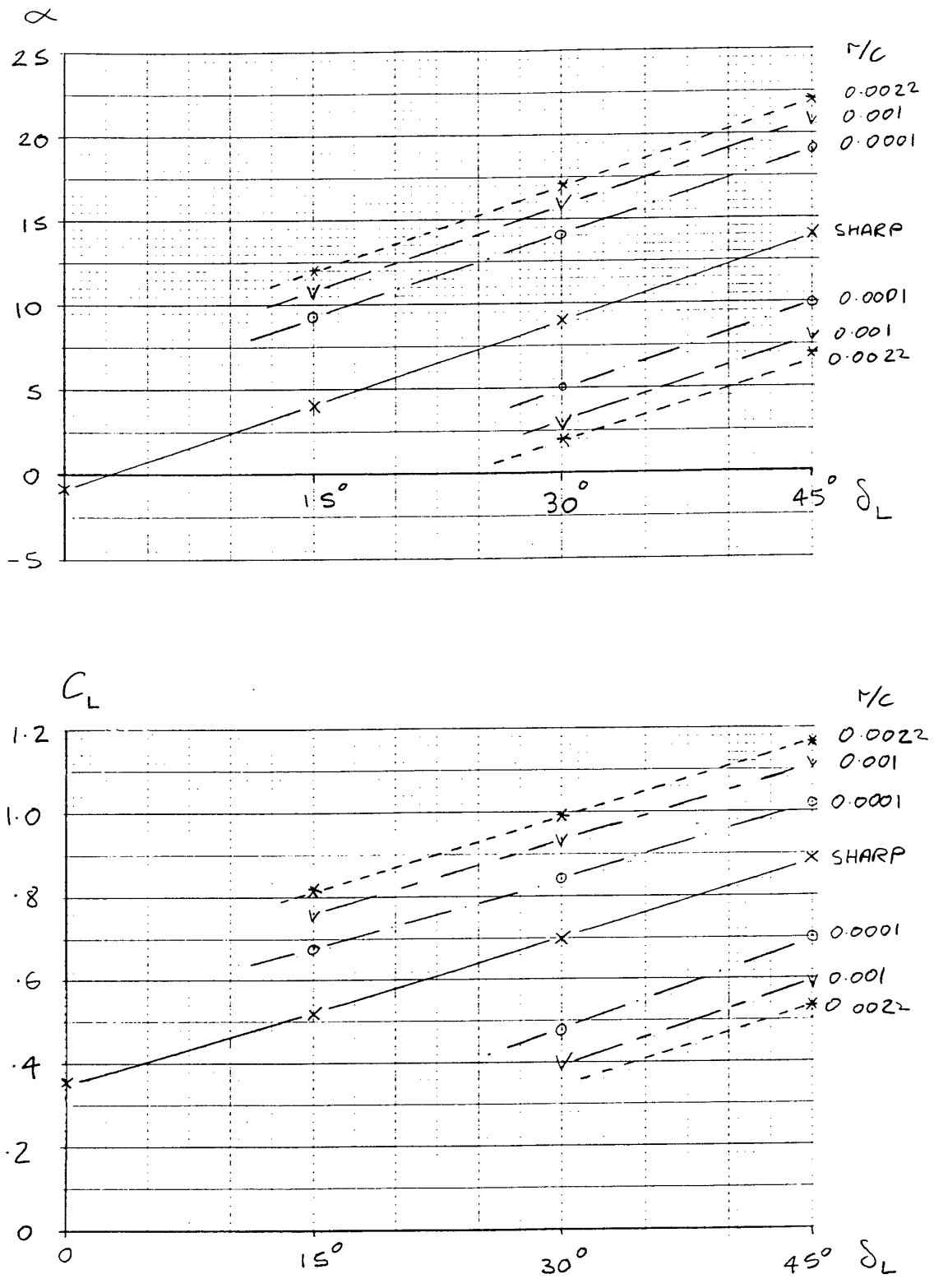

FIG. 3.18 (Cont'd) (c) $R = 20 \times 10^6$

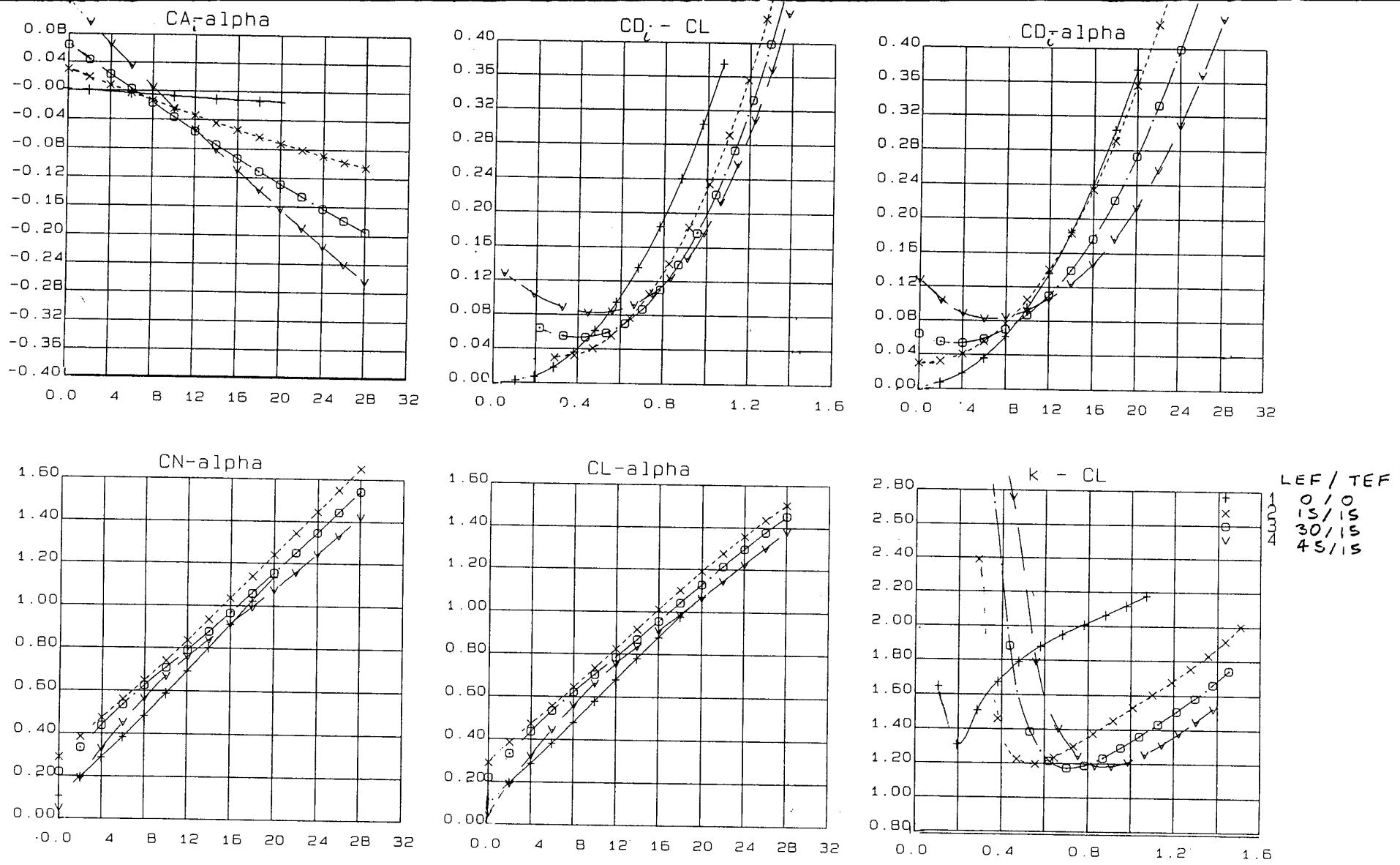

FIG. 3.19 PREDICTED RESULTS, BASIC WING WITH SHARP LE, LEF & TEF DEFLECTIONS, MACH 0.18

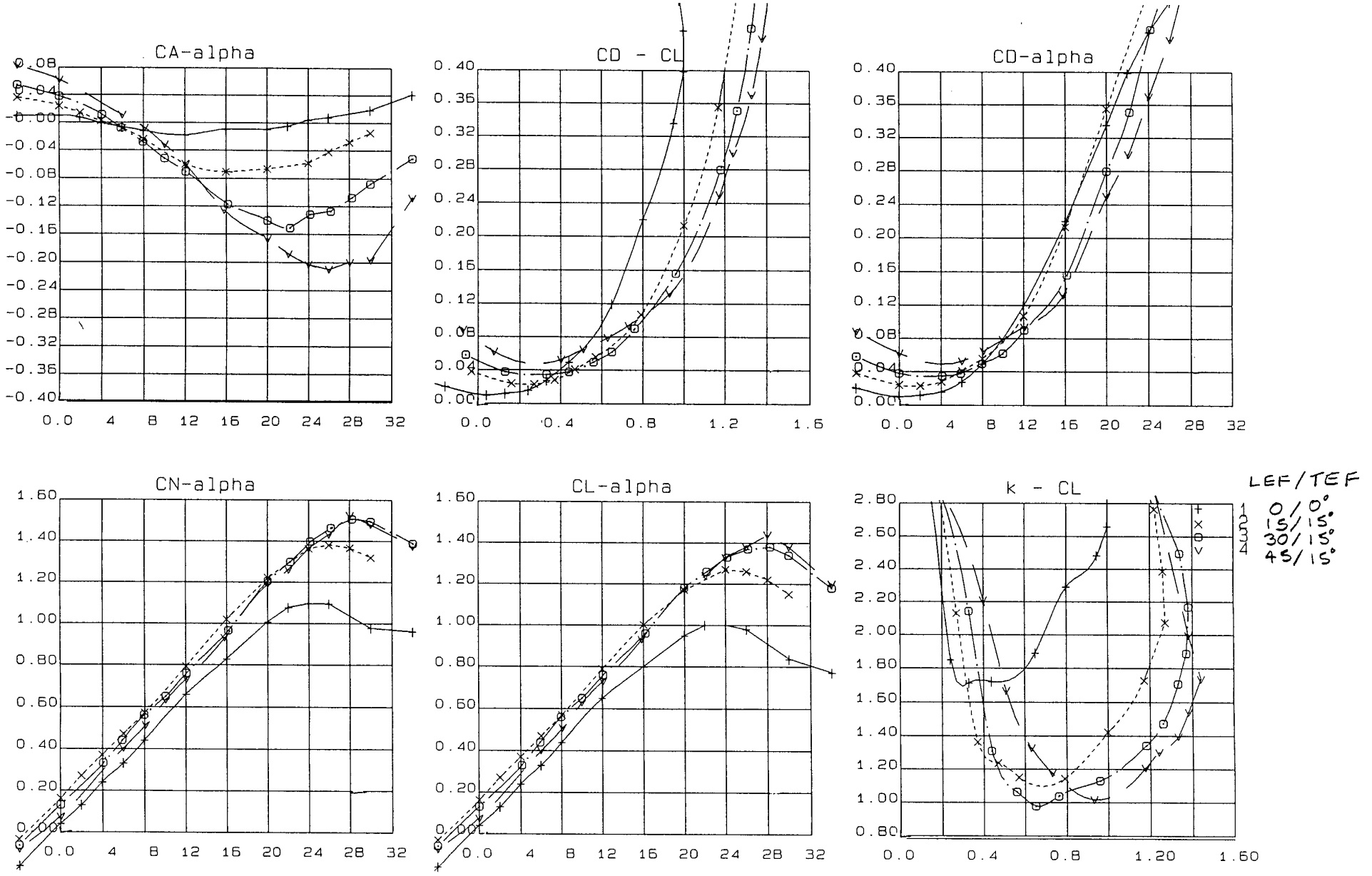

FIG. 3.20 EXPERIMENTAL RESULTS, BASIC WING WITH SHARP LE, LEF & TEF DEFLECTIONS, MACH 0.18, R = 5 x10^6

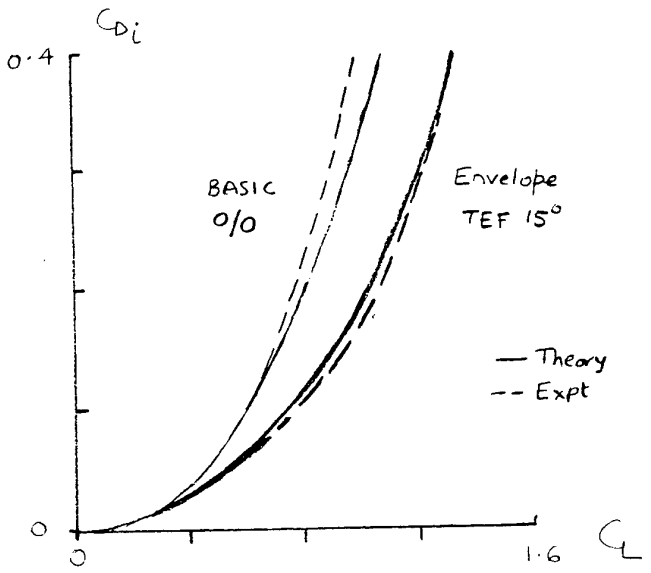

FIG. 3.21 BASIC WING WITH SHARP LE, LEF & TEF DEFLECTED, COMPARISON OF EXPERIMENTAL & PREDICTED LIFT-DRAG CHARACTERISTICS

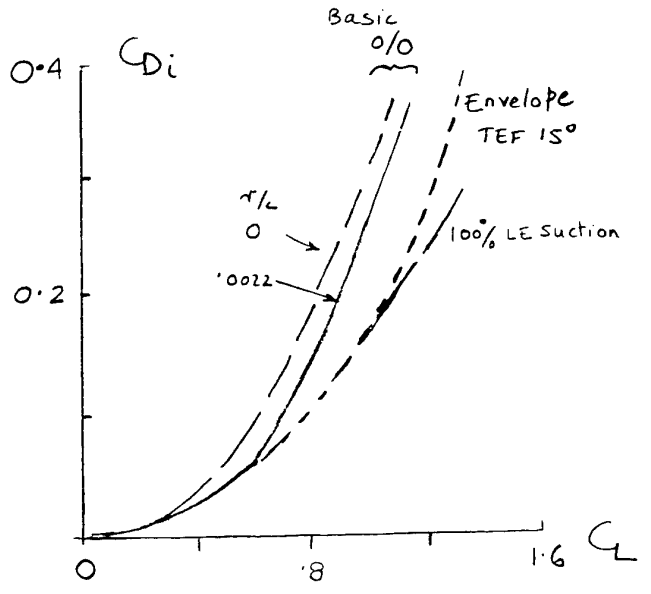

FIG. 3.22 BASIC WING WITH ROUNDED LE, LEF & TEF DEFLECTED, SUMMARISING THE LIFT-DRAG CHARACTERISTICS, r/c = 0.0022, MACH 0.18, R = 5 x10^6

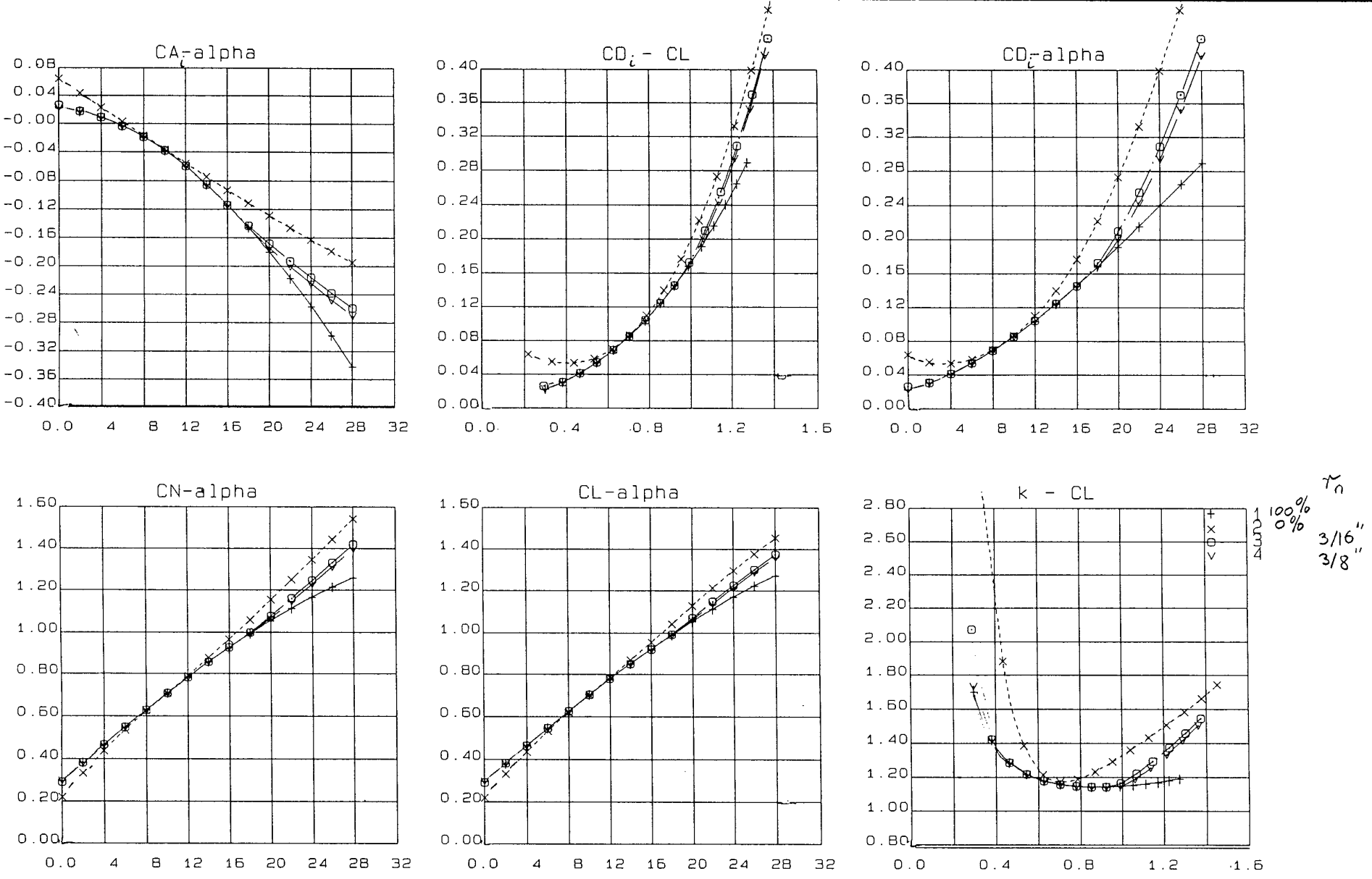

FIG. 3.23 BASIC WING, LEF 30° & TEF 15°, EFFECT OF LE RADIUS VARIATION, MACH 0.18, R = 5 x10⁶

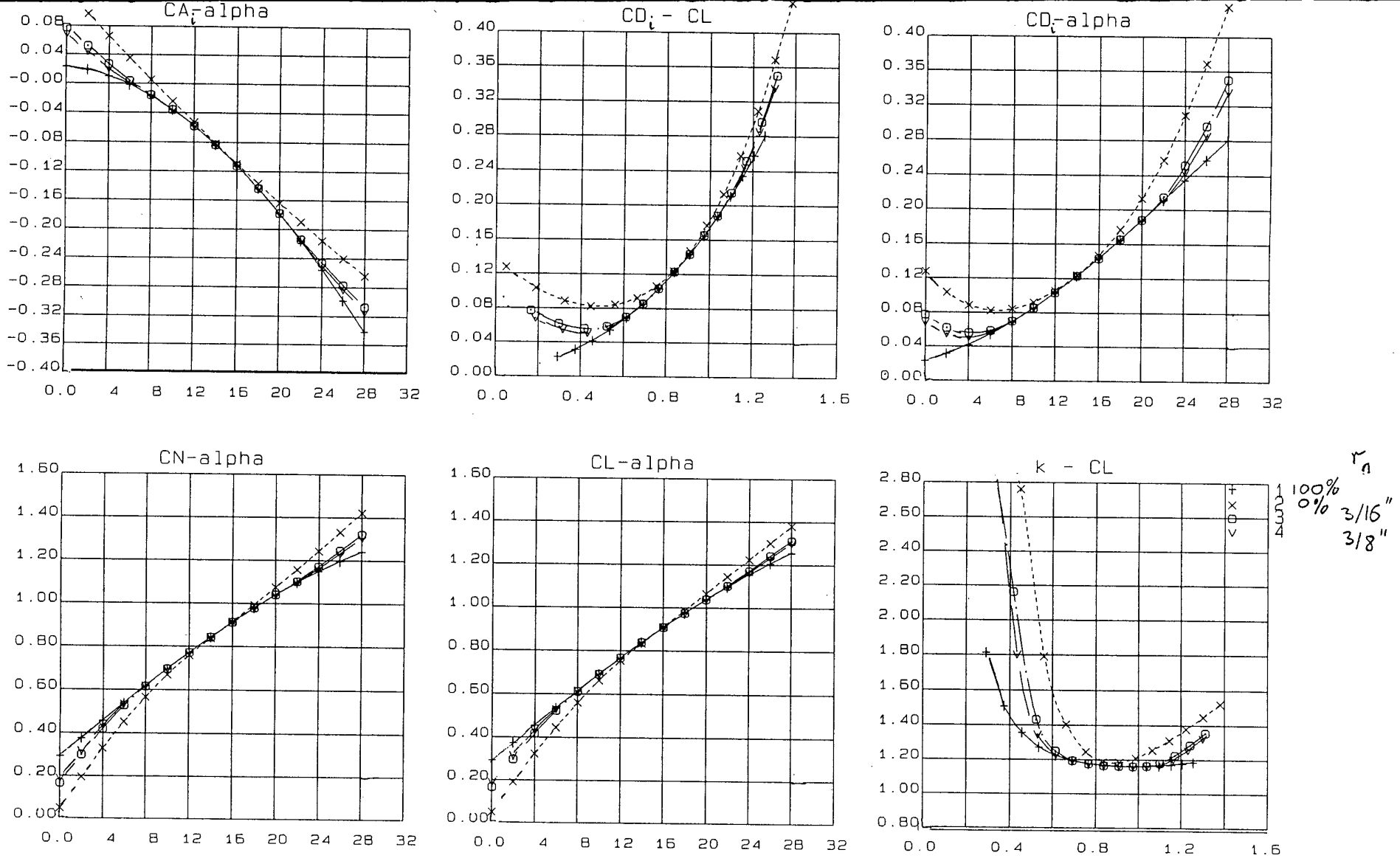

FIG. 3.24 BASIC WING, LEF 45° & TEF 15°, EFFECT OF LE RADIUS VARIATION, MACH 0.18, R = 5 x10⁶

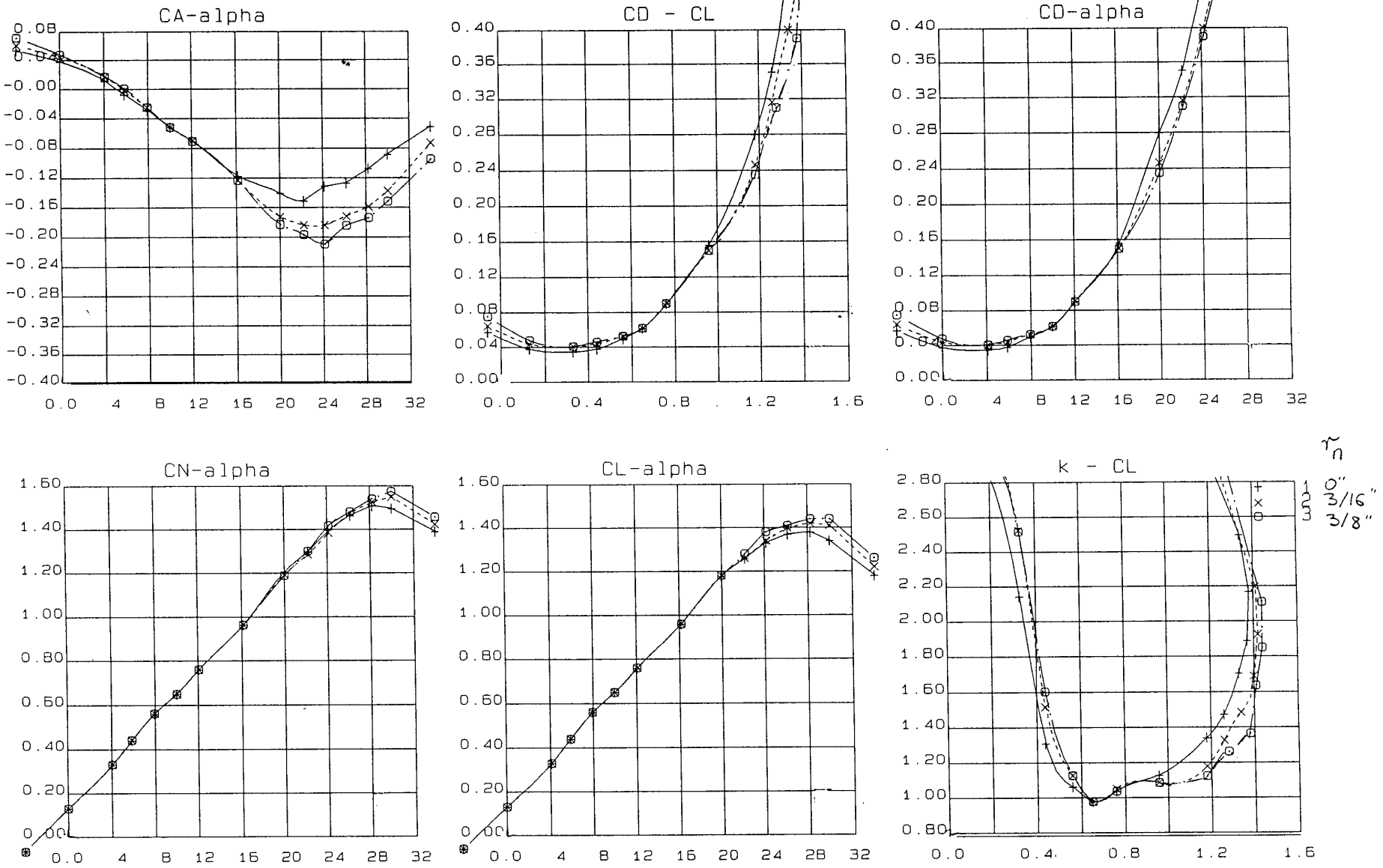

FIG. 3.25 EXPERIMENTAL RESULTS, BASIC WING WITH EFFECTS OF ROUNDED LE, LEF 30° & TEF 15°, MACH 0.18, R = 5 x10⁶

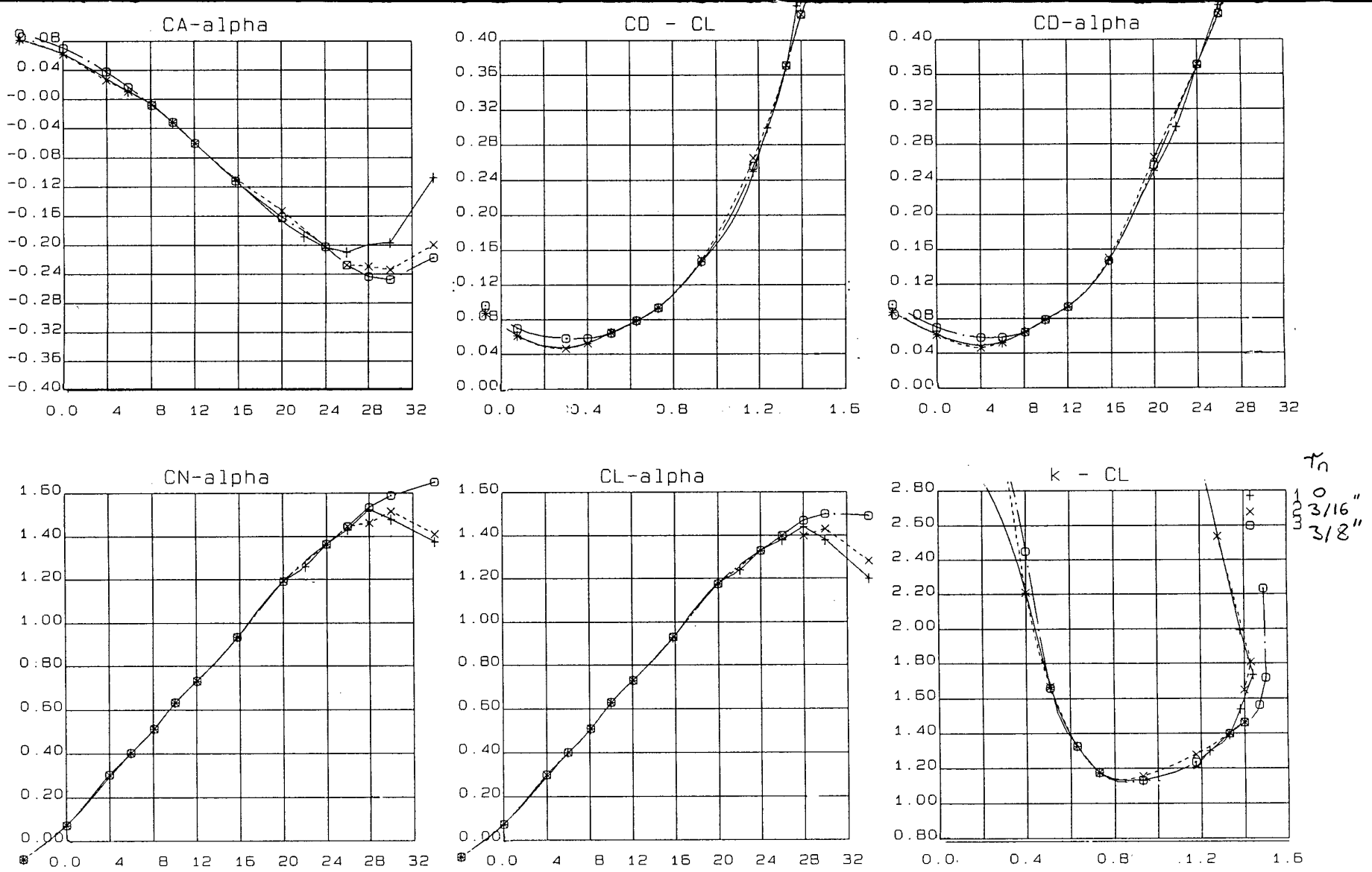

FIG. 3.26 EXPERIMENTAL RESULTS, BASIC WING WITH EFFECTS OF ROUNDED LE, LEF 45° & TEF 15°, MACH 0.18, R = 5 x10^6

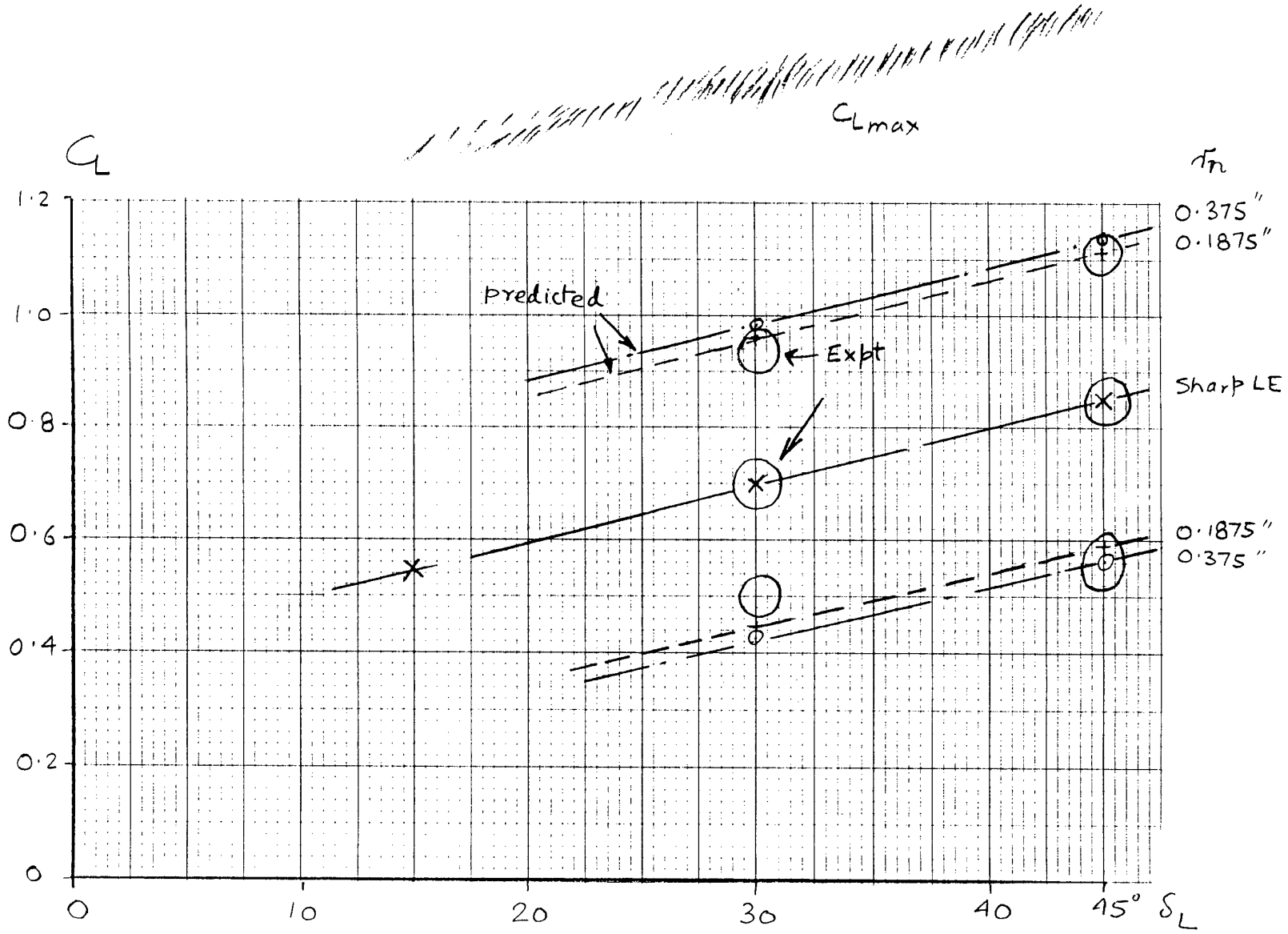

FIG. 3.27 WING WITH LEF & TEF DEFLECTION, COMPARISON OF PREDICTED & MEASURED ATTATCHED FLOW DOMAINS, C_L BASIS, EFFECT OF LE RADIUS VARIATION, MACH 0.18, R = 5 x10^6

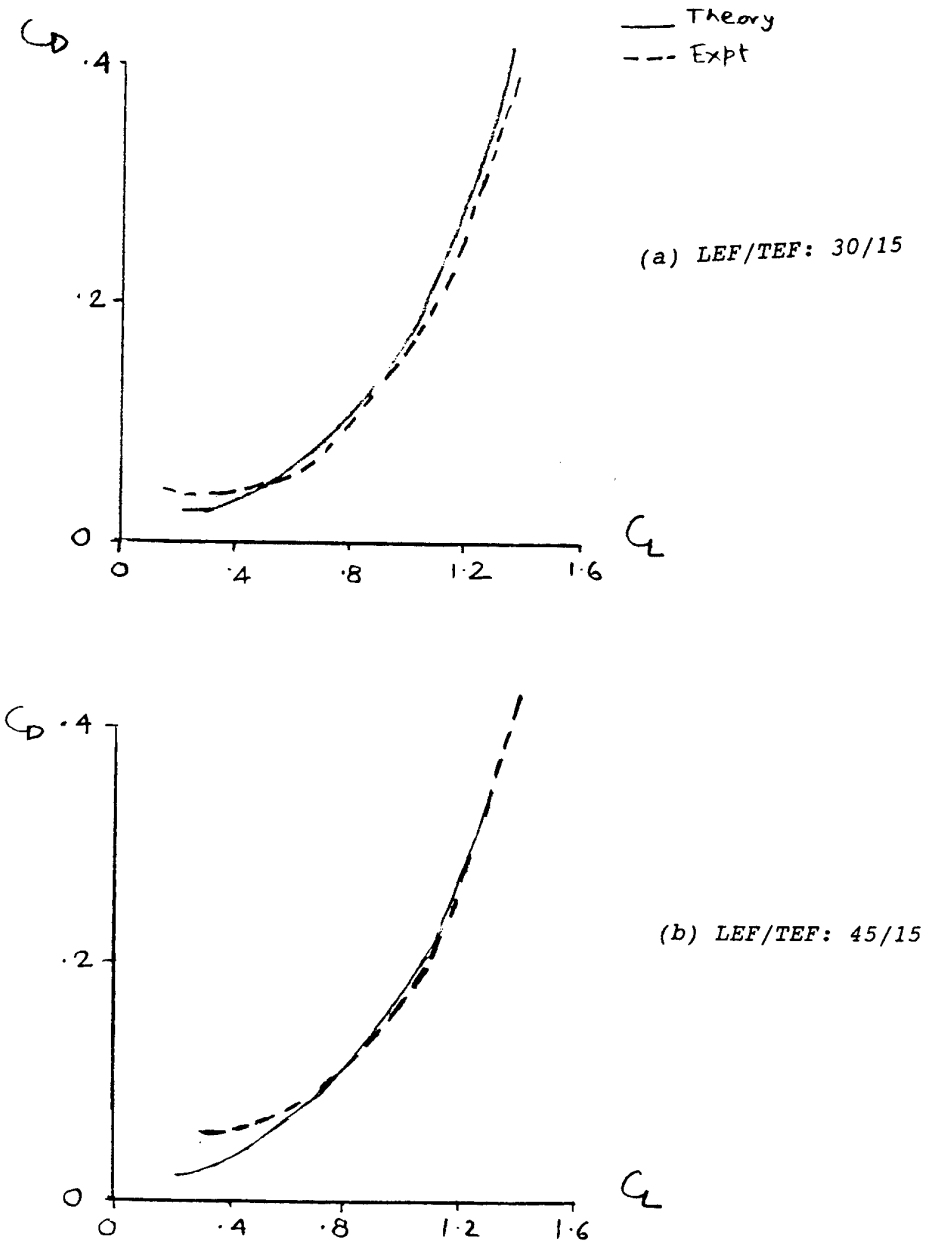

FIG. 3.28 COMPARING C_L - C_D FROM THEORY & EXPERIMENT FOR LEF/TEF: 30/15 & 45/15, r_n = 0.375", R = 5 x10^6

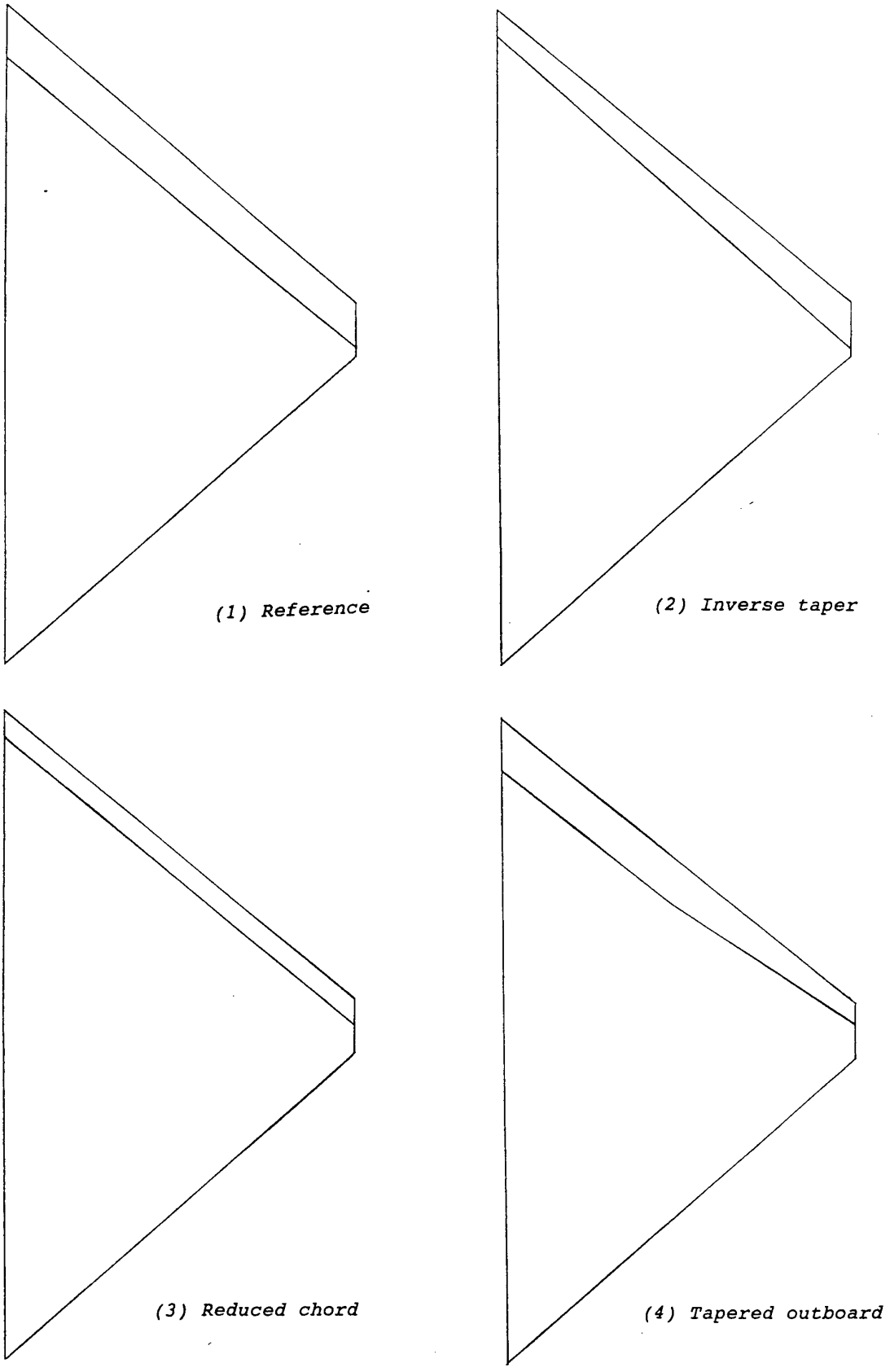

FIG. 4.1 POSSIBLE LEF CHORD VARIATION, HINGE-LINE (1) to (4)

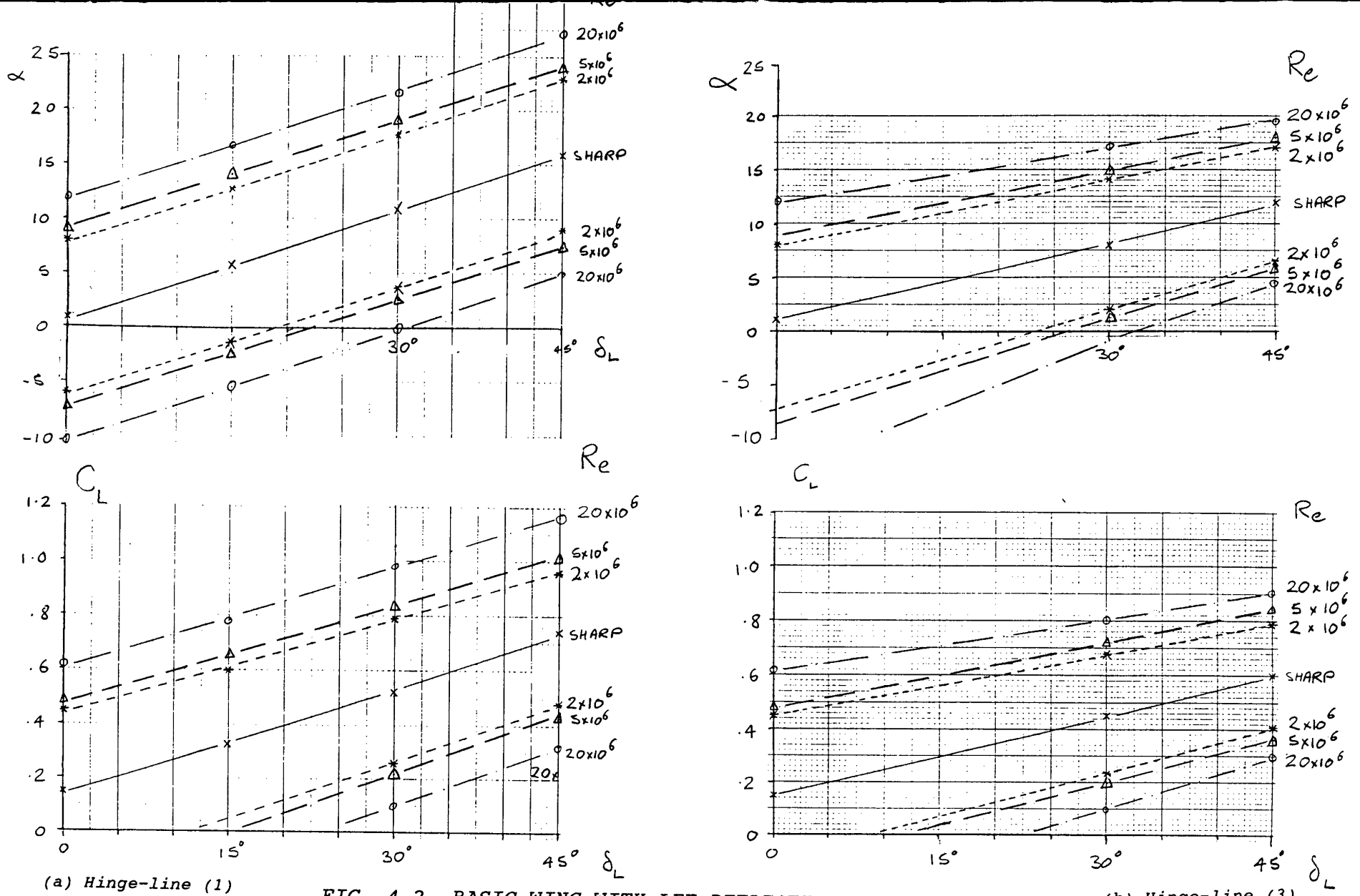

(a) Hinge-line (1)

(b) Hinge-line (3)

FIG. 4.2 BASIC WING WITH LEF DEFLECTION, TEF 0°, ATTACHED FLOW DOMAINS, α & C_L BASIS, EFFECT OF HINGE-LINE GEOMETRY CHANGES, MACH 0.18, R = 2, 5 & 20 x10^6, r/c = 0.0022

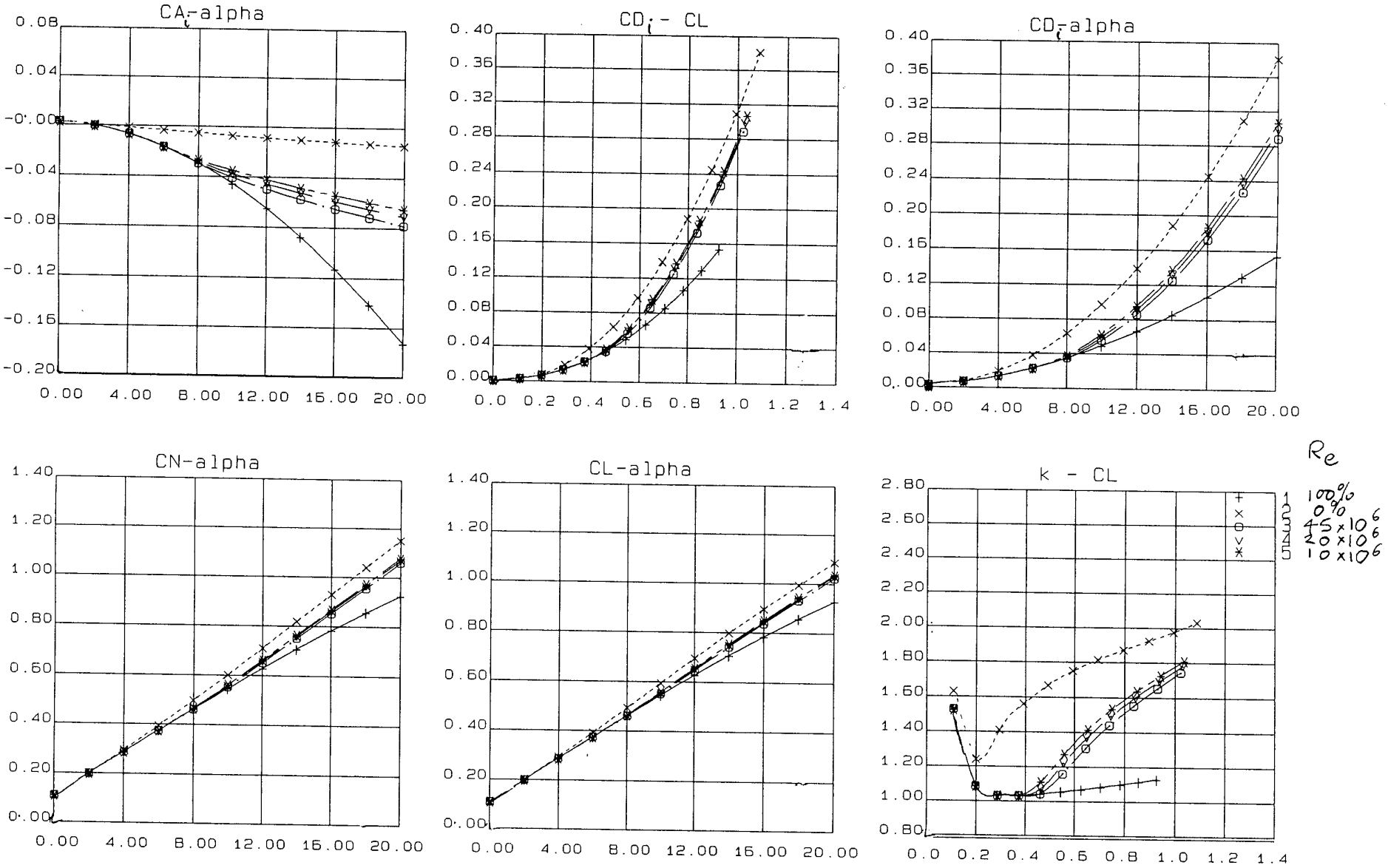

FIG. 5.1 BASIC WING, LE & TE FLAPS UNDEFLECTED, EFFECT OF R VARIATION, MACH 0.40, r/c = 0.0022

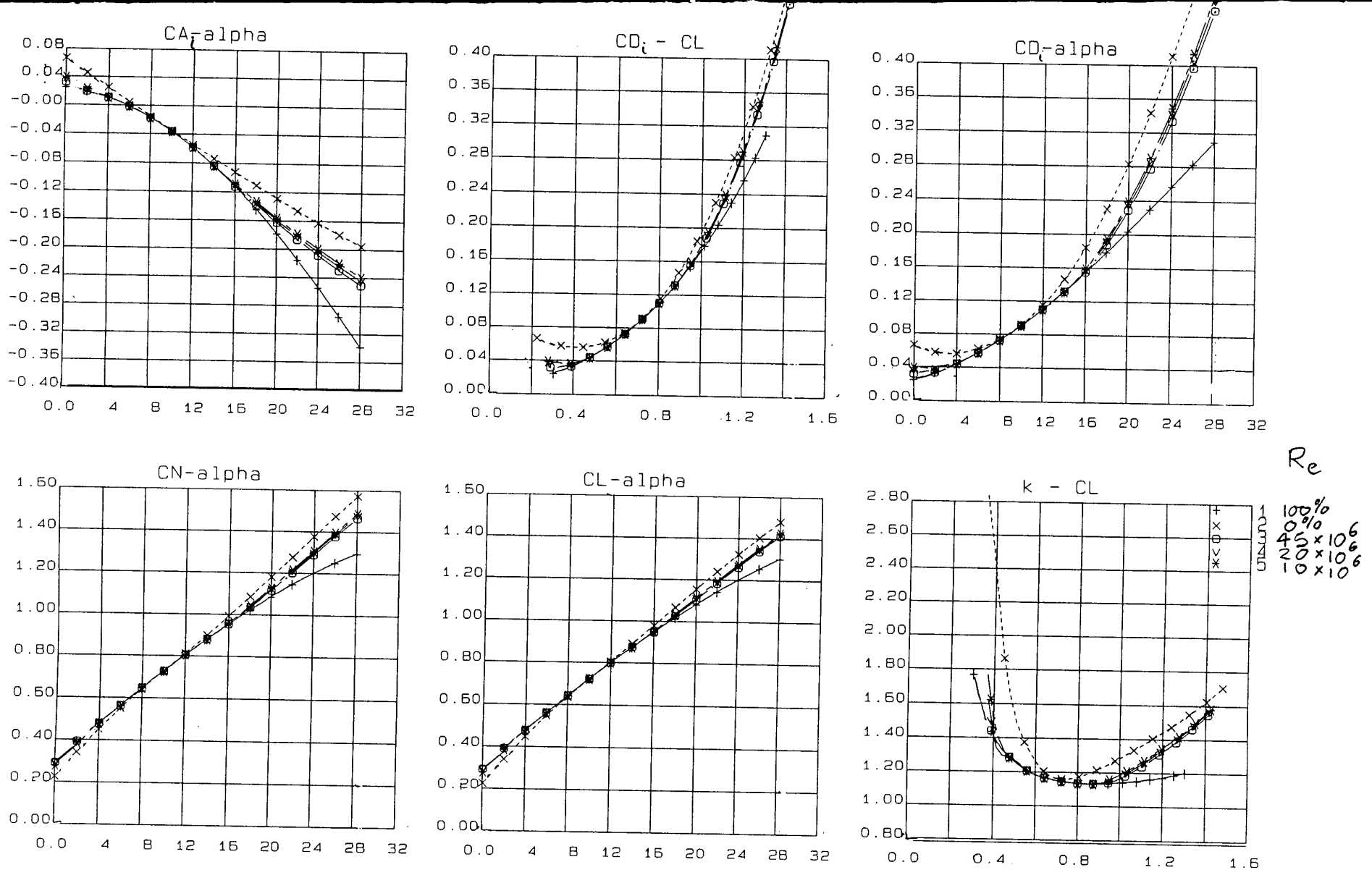

FIG. 5.2 BASIC WING, LEF 30° & TEF 15°, EFFECT OF R VARIATION, MACH 0.40, r/c = 0.0022

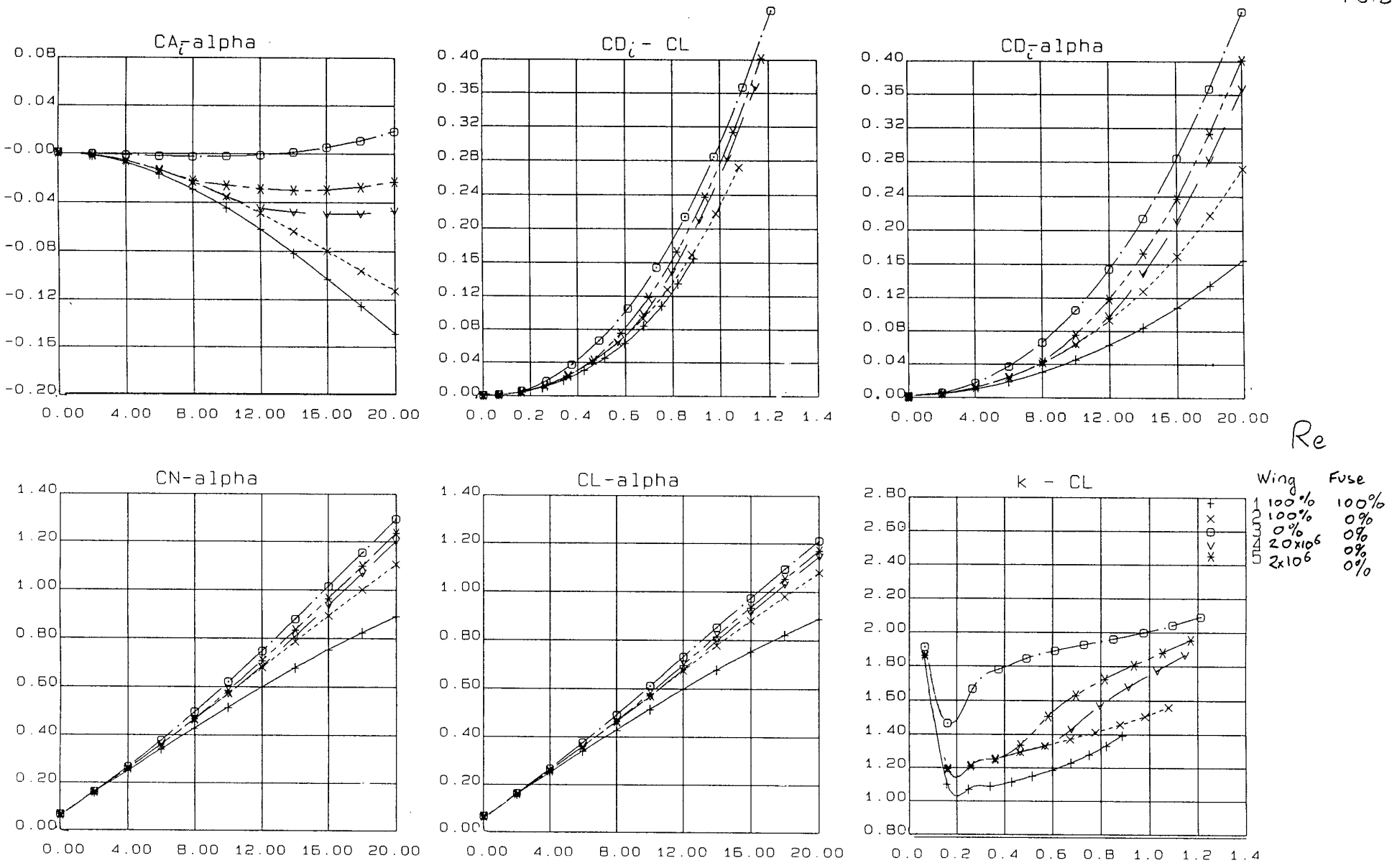

FIG. 6.1 PRELIMINARY WING+BODY RESULTS, LE & TE FLAPS UNDEFLECTED, EFFECT OF R VARIATION, MACH 0.18, r/c = 0.0022

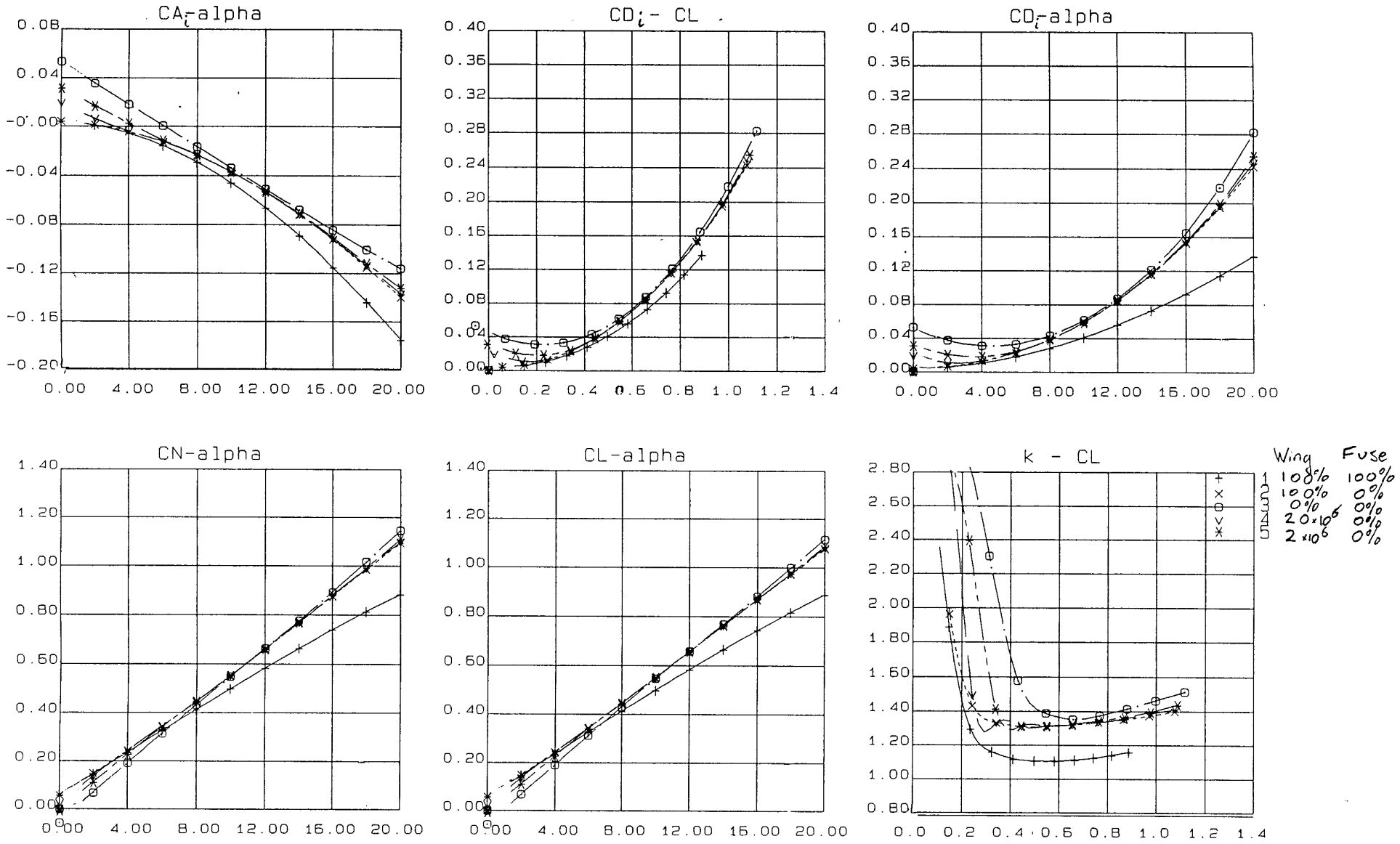

FIG. 6.2 PRELIMINARY WING+BODY RESULTS, LEF 30° & TEF 15°, EFFECT OF R VARIATION, MACH 0.18, r/c = 0.0022